

Profound synchrony of age-specific incidence rates and tumor suppression for different cancer types as revealed by the multistage-senescence model of carcinogenesis

Richard B. Richardson^{1,2}, Catalina V. Anghel³, Dennis S. Deng³

¹Radiobiology and Health Branch, Canadian Nuclear Laboratories (CNL), Chalk River Laboratories, Chalk River, ON K0J 1J0, Canada

²Medical Physics Unit, Cedars Cancer Centre, McGill University Health Centre - Glen Site, Montreal, QC H4A 3J1, Canada

³Computational Techniques Branch, Canadian Nuclear Laboratories (CNL), Chalk River Laboratories, Chalk River, ON K0J 1J0, Canada

Correspondence to: Richard B. Richardson; **email:** richard.richardson@cnl.ca

Keywords: aging, cancer incidence, cancer model, driver mutations, SEER program

Received: June 17, 2021

Accepted: September 7, 2021

Published: October 25, 2021

Copyright: © 2021 Richardson et al. This is an open access article distributed under the terms of the [Creative Commons Attribution License](https://creativecommons.org/licenses/by/3.0/) (CC BY 3.0), which permits unrestricted use, distribution, and reproduction in any medium, provided the original author and source are credited.

ABSTRACT

The age-specific trend of cancer incidence rates, but not its magnitude, is well described employing the multistage theory of carcinogenesis by Armitage and Doll in combination with the senescence model of Pompei and Wilson. We derived empirical parameters of the multistage-senescence model from U.S. Surveillance, Epidemiology, and End Results (SEER) incidence data from 2000–2003 and 2010–2013 for The Cancer Genome Atlas (TCGA) cancer types. Under the assumption of a constant tumor-specific transition rate between stages, there is an extremely strong linear relationship ($P < 0.0001$) between the number of stages and the stage transition rate. The senescence tumor suppression factor for 20 non-reproductive cancers is remarkably consistent (0.0099 ± 0.0005); however, five female reproductive cancers have significantly higher tumor suppression. The peak incidence rate for non-reproductive cancers occurs at a younger age for cancers with fewer stages and their carcinogenic stages are of longer duration. Driver gene mutations are shown to contribute on average only about a third of the carcinogenic stages of different tumor types. A tumor's accumulated incidence, calculated using a two-variable (age, stage) model, is strongly associated with intrinsic cancer risk. During both early adulthood and senescence, the pace of tumor suppression appears to be synchronized across most cancer types, suggesting the presence of overlapping evolutionary processes.

INTRODUCTION

Cancer incidence rates in adults generally rise exponentially with post-pubertal age, peak around 80 years, and then approach zero after age 100, although estimates are higher in centenarians if incidental tumors discovered at autopsy are included [1]. Mortality rates show a similar age-dependent trend delayed by survival, the time from clinical manifestation of the cancer until death [2, 3].

For most cancers in adults, the rise in the age-specific rate of cancer incidence $ASR(t)$ can be represented by probabilities of occurrence of successive independent stages and by a power function [4]. The probability per unit time of the i^{th} stage occurring, up to a total of k stages can be denoted by p_i . Using the notation and simplification described in the review by Frank [5], we assume that for each cancer, these probabilities are equal ($p_1 = p_2 = \dots = p_k = u$). Therefore, if each stage of a unicellular or multicellular process proceeds at a small,

roughly constant stage-transition rate u per year, the probability of any step occurring after t years is $1 - e^{-ut} \approx ut$. At age t the probability that $k-1$ steps have occurred is approximately $(ut)^{k-1}$, and the final stage-transition rate is u (yr^{-1}); therefore, the approximate rate (incidence) of occurrence at time t is

$$ASR(t) = (p_1 p_2 \dots p_k) t^{k-1} = u^k \cdot t^{k-1} \quad 1)$$

Nordling [6] and Armitage and Doll [7] accounted for and modeled age-related cancer incidence as a power function that is dependent on a discrete number of ordered sequential stages:

$$ASR(t) = u^k / (k-1)! \cdot t^{k-1} \quad 2)$$

Generalizing the factorial function to the gamma function as $\Gamma(k) = (k-1)!$ for natural numbers k ,

$$ASR(t) = u^k / \Gamma(k) \cdot t^{k-1} \quad 3)$$

To accommodate the old age decline in this multistage power function, Pompei and Wilson [8] developed their “beta model” of senescence, in which the empirical tumor suppression term $(1-bt)$, with $0 \leq t \leq b^{-1}$, is based on the linear decline in cellular senescence or cell population doubling b (yr^{-1}) and is equal to unity at birth for cancers of non-reproductive organs (henceforth referred to as “non-reproductive cancers”), or alternatively around the time of puberty, 15 years, for cancers of reproductive organs or “reproductive cancers”. Thus, t represents age for non-reproductive cancers, and $(\text{age} - 15) \geq 0$ for reproductive cancers.

$$ASR(t) = a \cdot t^{k-1} \cdot (1-bt), \text{ with } 0 \leq t \leq b^{-1} \quad 4)$$

Senescence tumor suppressor b (yr^{-1}) is a constant parameter and a is a variable parameter that can be substituted according to Equation 3:

$$ASR(t) = u^k / \Gamma(k) \cdot t^{k-1} \cdot (1-bt) = A \cdot B \cdot C \quad 5)$$

where A is the “stage-transition-rate tumor suppression” term that is age-independent and exponential, B is an age-dependent “power law” growth term, and C is an age-dependent linear “senescence tumor suppression” term.

Harding et al. [9] produced best fit curves of the multistage-senescence model to U.S. Surveillance, Epidemiology, and End Results (SEER) program age-specific cancer incidence for three decades of data (1979–1983, 1989–1993, and 1999–2003). In a similar manner, we investigate the multistage-senescence model of carcinogenesis and model-fit to the age-specific rate

of cancer incidence from SEER data sets for 2000–2003 and 2010–2013 [10] of The Cancer Genome Atlas (TCGA) cancer types [9, 11]. We show that just two variables (age and the number of carcinogenic stages) have a major influence, not only on the trend, but on the magnitude of age-specific incidence rate for all cancer types analyzed. In addition, the multistage-senescence model of carcinogenesis indicates that the number of stages is positively related to the age of peak incidence rate and inversely related to the stage-transition rate. Finally, the U.S. SEER data were matched to the cancer types from the National Cancer Institute TCGA data set to allow an estimate of the proportion of the total number of stages associated with driver gene mutations.

RESULTS

The age-specific rate of cancer incidence was estimated following the methods of Harding et al. [9] from U.S. Census data [12] and the SEER cancer registry data for 2000–2003 and 2010–2013 [10] of 23 non-reproductive cancers as well as five female-specific cancers and two male-specific cancers. The parameters values are given in Table 1A–1C for geometric mean of the stage-transition rate u , senescence tumor suppressor b , and stages k for the weighted model-fits to SEER 2010–2013 incidence rates employing the multistage-senescence model (Equation 5) for males and females separately as well as for both sexes pooled. We will use the terms “both” or “both sexes pooled” to refer to the case when all incidence cases (both male and female, M&F) of non-reproductive cancer types were considered and corresponding estimates produced. We will use the term “male” when male-only cancer incidence data (both reproductive and non-reproductive) were tabulated and analyzed to produce estimates, and analogously for “female.” When we refer to “male and female,” the estimates were produced separately for males and females and the estimates (not the incidence data) were pooled. Exact probability P values are given unless the statistical test is insignificant when applying multiple testing correction.

Results from 2010–2013 are presented in this section and in Supplementary Table 1A–1C, whereas the similar results for 2000–2003 are found only in Supplementary Table 2A–2C. Unless stated otherwise, significant results hold for both the 2000–2003 and 2010–2013 data sets. Cancers having P values for model-fitted u or k larger than 0.1 were omitted from further analysis (Supplementary Table 1A–1C). Thus, for 2010–2013, glioma, LGG and neuroendocrine tumors, PCPG (TCGA abbreviations defined in Table 1A, 1B footnotes) were omitted from further analysis, as well as rectal cancer, READ for females. For the years 2000–2003, LGG and PCPG were omitted as well as adrenal cancer, ACC for

Table 1A. Male (M) parameter values of model-fits to SEER 2010–2013 age-specific cancer incidence rates for reproductive and non-reproductive cancer types, employing the multistage-senescence model (Equation 5).

Sex	Cancer type (TCGA) ⁰	Model-fitted ¹			Peak incidence rate (per 100,000 person-year)		Age of peak incidence (yr)		Cumulative probability over lifespan			Ratio of cum. prob., SEER/2-variable
		u_{μ} (yr ⁻¹)	k	b (yr ⁻¹)	SEER	Model-fitted ²	SEER	Model-fitted ³	SEER	Model-fitted ⁴	2-Variable model fitted	
M	ACC	0.011	6.44	0.0107	0.347	0.301	87.5	79.2	0.00012	9.50E-05	0.010	0.011
M	BLCA	0.040	9	0.0098	344	380	92.5	91.0	0.10	0.10	0.017	6.1
M	COAD	0.029	6.9	0.0094	228	230	92.5	90.9	0.08	0.078	0.023	3.5
M	COADREAD	0.027	6.19	0.0092	274	279	92.5	91.2	0.10	0.11	0.026	3.9
M	ESCA	0.025	6.91	0.0101	42.5	47.4	82.5	84.9	0.016	0.015	0.014	1.1
M	GBM	0.019	6.16	0.0103	19.7	19.3	77.5	81.7	0.0067	0.0065	0.013	0.5
M	HNSC	0.019	5.07	0.0100	110	90.4	102.5	80.6	0.041	0.037	0.017	2.4
M	KICH	0.014	5.88	0.0106	4.13	3.65	72.5	78.2	0.0013	0.0012	0.011	0.12
M	KIRC	0.017	5.13	0.0105	41.9	37.9	72.5	76.9	0.014	0.014	0.013	1.0
M	KIRP	0.016	5.62	0.0106	13.5	11.4	72.5	77.2	0.0039	0.004	0.011	0.34
M	LAML	0.030	8.37	0.0098	42.0	45.5	87.5	89.5	0.014	0.013	0.016	0.85
M	LGG	9.20E-05	1.52	0.0085	0.502	0.363	82.5	40.3	0.0003	0.00030	0.032	0.0094
M	LIHC	0.015	4.57	0.0102	47.3	46.1	62.5	76.7	0.018	0.020	0.017	1.1
M	LUAD	0.035	7.81	0.0102	202	206	82.5	85.6	0.059	0.058	0.012	4.8
M	LUSC	0.035	8.4	0.0102	135	134	82.5	85.9	0.036	0.036	0.011	3.1
M	MESO	0.038	11.42	0.0100	11.0	12.7	92.5	91.5	0.0027	0.0027	0.014	0.19
M	PAAD	0.027	7.09	0.0101	74.9	75.7	82.5	85.1	0.023	0.023	0.014	1.7
M	PCPG	7.00E-06	1.33	-0.0168	0.407	NaN	92.5	-14.8	9.30E-05	NaN	NaN	NaN
M	READ	0.014	4.49	0.0089	51.0	49.9	97.5	87.8	0.023	0.025	0.031	0.73
M	SARC	0.015	6.4	0.0071	12.6	24.4	87.5	119	0.0042	0.012	0.13	0.031
M	SKCM	0.027	6.52	0.0093	220	195	102.5	91.0	0.075	0.070	0.024	3.1
M	STAD	0.026	7.24	0.0096	71.4	70.2	97.5	90.2	0.024	0.023	0.020	1.2
M	THCA	0.011	4.14	0.0103	19.8	18.3	72.5	73.6	0.0087	0.0082	0.017	0.52
M	THYM	0.012	6.11	0.0107	1.00	0.795	82.5	78.1	0.00028	0.00026	0.010	0.027
M	PRAD	0.035	5.11	0.0125	746	642	72.5	79.5	0.22	0.21	0.0055	40
M	TGCT	0.0013	1.52	0.0237	14.7	12.5	27.5	29.3	0.0040	0.0036	0.0067	0.60

⁰Non-reproductive cancers: ACC adrenocortical carcinoma, BLCA bladder urothelial carcinoma, COAD colon adenocarcinoma, COADREAD both COAD and READ cases, ESCA esophageal carcinoma, GBM glioblastoma multiforme, HNSC head and neck squamous cell carcinoma, KICH kidney chromophobe, KIRC kidney renal clear cell carcinoma, KIRP kidney renal papillary cell carcinoma, LAML acute myeloid leukemia, LGG brain lower grade glioma, LIHC liver hepatocellular carcinoma, LUAD lung adenocarcinoma, LUSC lung squamous cell carcinoma, MESO mesothelioma, PAAD pancreatic adenocarcinoma, PCPG pheochromocytoma and paraganglioma, READ rectum adenocarcinoma, SARC sarcoma, SKCM skin cutaneous melanoma, STAD stomach adenocarcinoma, THYM thymoma, THCA thyroid carcinoma.

Male reproductive cancers: PRAD prostate adenocarcinoma, TGCT testicular germ cell tumors.

Other abbreviations: NaN Not a Number.

¹Equation 5; ²Equation 6; ³Equation 6 substituted in Equation 5; ⁴Equation 7.

The peak age-specific incidence rate, age of peak incidence rate, and cumulative probability of cancer over life span are computed up to maximum age 105, based on the SEER data alternatively model-fitted $ASR(t)$. The age-specific incidence rate is computed per 100,000 population for each five-year age group. LGG and PCPG are cancer types with P values for model-fitted u_{μ} or k larger than 0.1 and were omitted from further analysis (see Supplementary Table 1A–1C).

females and both sexes, and sarcoma, SARC for females only. In addition, colorectal cancer COADREAD was omitted from some analyzes, such as from comparisons of b and k values, and from regression lines, when

COAD and READ cases were included instead. Therefore, there are 20 and 19 paired cancer types for males and females for the 2010–2013 and 2000–2003 data, respectively.

Table 1B. Female (F) parameter values of model-fits to SEER 2010–2013 age-specific cancer incidence rates for reproductive and non-reproductive cancer types, employing the multistage-senescence model (Equation 5).

Sex	Cancer type (TCGA) ⁰	Model-fitted ¹			Peak incidence rate (per 100,000 person-year)		Age of peak incidence (yr)		Cumulative probability over lifespan			Ratio of cum. prob., SEER/2-variable
		u_{μ} (yr ⁻¹)	k	b (yr ⁻¹)	SEER	Model-fitted ²	SEER	Model-fitted ³	SEER	Model-fitted ⁴	2-Variable model fitted	
F	ACC	0.005	4.42	0.0105	0.396	0.343	77.5	73.7	0.00015	0.00014	0.0077	0.02
F	BLCA	0.030	8.08	0.0097	64.6	72.7	92.5	90.2	0.022	0.021	0.0071	3.1
F	COAD	0.030	7.23	0.0095	193	188	87.5	90.2	0.062	0.061	0.0086	7.2
F	COADREAD	0.028	6.55	0.0093	220	213	87.5	90.6	0.075	0.076	0.010	7.1
F	ESCA	0.020	7.09	0.0098	11.7	12.1	87.5	88.1	0.0043	0.0039	0.0075	0.58
F	GBM	0.015	5.56	0.0101	12.6	11.1	77.5	81.4	0.0042	0.0042	0.0075	0.56
F	HNSC	0.015	5.13	0.0092	31.4	29.5	92.5	87.1	0.013	0.013	0.013	1.0
F	KICH	0.0083	4.74	0.0104	2.21	1.86	77.5	75.6	0.00081	0.00075	0.0074	0.11
F	KIRC	0.013	4.63	0.0104	23.2	18	72.5	75.6	0.0073	0.0075	0.0078	0.94
F	KIRP	0.011	5.22	0.0105	3.56	2.98	77.5	77.3	0.0011	0.0011	0.0065	0.17
F	LAML	0.023	7.33	0.0097	22.0	23.1	82.5	88.8	0.0082	0.0072	0.0075	1.1
F	LGG	0.00093	2.65	0.0101	0.364	0.213	32.5	61.4	0.00022	0.00013	0.013	0.017
F	LIHC	0.018	6.06	0.0101	17.3	16.2	82.5	82.4	0.0057	0.0056	0.0067	0.85
F	LUAD	0.029	6.73	0.0101	162	144	77.5	84.0	0.047	0.046	0.0060	7.8
F	LUSC	0.028	7.65	0.0102	69.0	51.9	77.5	85.3	0.016	0.015	0.0051	3.1
F	MESO	0.018	7.85	0.0091	2.29	2.15	102.5	96.3	0.00065	0.00068	0.012	0.052
F	PAAD	0.027	7.18	0.0100	60.7	59.5	82.5	86.0	0.019	0.018	0.0062	3.0
F	PCPG	0.004	4.45	0.0109	0.182	0.111	72.5	71.1	6.10E-05	4.50E-05	0.0064	0.0094
F	READ	0.0043	2.82	0.0038	28.3	49.3	82.5	170	0.013	0.076	0.20	0.063
F	SARC	0.0093	5.01	0.0077	7.67	6.65	97.5	104	0.0023	0.0035	0.031	0.074
F	SKCM	0.012	4.08	0.0083	59.4	58.8	82.5	91.0	0.029	0.033	0.022	1.3
F	STAD	0.022	6.98	0.0094	34.4	33.1	102.5	91.2	0.012	0.011	0.0099	1.2
F	THCA	0.0053	2.36	0.0102	38.3	36.6	52.5	56.3	0.022	0.022	0.013	1.7
F	THYM	0.0087	5.34	0.0107	0.793	0.658	67.5	75.7	0.00025	0.00024	0.0056	0.045
F	BRCA	0.023	3.72	0.0115	435	428	77.5	78.5	0.19	0.18	0.0065	30
F	CESC	0.0011	1.57	0.0105	13.8	11.9	42.5	49.5	0.0071	0.0078	0.0094	0.76
F	OV	0.011	4.07	0.0121	12.7	11.9	72.5	77.5	0.0045	0.0046	0.0048	0.96
F	UCEC	0.013	3.4	0.0121	84.0	73.1	67.5	73.2	0.03	0.032	0.0061	5.0
F	UCS	0.010	5.59	0.0125	0.711	0.519	82.5	80.6	0.00018	0.00016	0.0022	0.081

⁰Female reproductive cancers: BRCA breast invasive carcinoma, CESC cervical squamous cell carcinoma and endocervical adenocarcinoma, OV ovarian serous cystadenocarcinoma, UCEC uterine corpus endometrial carcinoma, UCS uterine carcinosarcoma.

Abbreviations for non-reproductive cancer types and footnotes 1-4 are explained in Table 1A. LGG, PCPG and READ are cancer types with *P* values for model-fitted u_{μ} or k larger than 0.1 and were omitted from further analysis.

Senescence tumor suppressor

We fit the multistage-senescence model (Equation 5) to cancer incidence rate and analyzed the trends in the senescence tumor suppressor b , a parameter linked to declining cancer rates in very old age, with sex and different cancer types. There is insignificant variation (when adjusted for multiple testing) in b (yr⁻¹) for non-reproductive cancers between sexes, according to the paired *t* test, with the b value for female cancers on average only about 2% smaller than that for males for the same cancer ($n = 20$, $P > 0.1$, Holm method). The

mean b value for female non-reproductive cancers is 0.0098 ± 0.0008 (SD, $n = 20$) and for males it is 0.0100 ± 0.0008 (SD, $n = 20$, omitting rectal cancer, READ to compare paired values). The mean value of b for non-reproductive cases of both sexes pooled, omitting READ, is 0.0100 ± 0.0005 (SD, $n = 20$), and 0.00991 ± 0.0006 (SD, $n = 21$) including READ.

The mean value of b for all (non-reproductive and reproductive) male cancers is 0.0106 ± 0.0030 (SD, $n = 23$, Table 1A, males) and for females 0.0102 ± 0.0011 (SD, $n = 25$, Table 1B, females). We also performed

Table 1C. Both sexes pooled (M&F) parameter values of model-fits to SEER 2010–2013 age-specific cancer incidence rates for non-reproductive cancer types only, employing the multistage-senescence model (Equation 5).

Sex	Cancer type (TCGA) ⁰	Model-fitted ¹			Peak incidence rate (per 100,000 person-year)		Age of peak incidence (yr)		Cumulative probability over lifespan			Ratio of cum. prob., SEER/2-variable
		u_{μ} (yr ⁻¹)	k	b (yr ⁻¹)	SEER	Model-fitted ²	SEER	Model-fitted ³	SEER	Model-fitted ⁴	2-Variable model fitted	
M&F	ACC	0.0067	5.1	0.0105	0.329	0.319	77.5	76.6	0.00014	0.00012	0.0064	0.021
M&F	BLCA	0.036	8.47	0.0098	161	183	87.5	89.6	0.052	0.050	0.013	4.1
M&F	COAD	0.030	7.03	0.0095	203	203	87.5	90.1	0.068	0.067	0.014	5.0
M&F	COADREAD	0.027	6.32	0.0093	238	235	87.5	90.2	0.084	0.086	0.014	6.0
M&F	ESCA	0.022	6.64	0.0100	24.1	26	82.5	84.7	0.009	0.0085	0.0092	0.98
M&F	GBM	0.016	5.65	0.0101	15.7	14.3	77.5	81.6	0.0052	0.0053	0.0082	0.63
M&F	HNSC	0.017	4.87	0.0098	52.6	54.3	77.5	80.9	0.024	0.023	0.0088	2.7
M&F	KICH	0.010	5.17	0.0105	3.05	2.58	72.5	77.0	0.001	0.00098	0.0065	0.16
M&F	KIRC	0.014	4.69	0.0104	31.7	26.1	72.5	75.8	0.010	0.011	0.0066	1.5
M&F	KIRP	0.012	5.05	0.0105	8.04	6.33	72.5	76.4	0.0024	0.0024	0.0064	0.37
M&F	LAML	0.026	7.77	0.0098	29.6	31.4	82.5	88.8	0.010	0.0093	0.012	0.85
M&F	LGG	0.00064	2.34	0.0099	0.404	0.279	32.5	57.9	0.00026	0.00018	0.0026	0.10
M&F	LIHC	0.014	4.69	0.0102	28.4	28.7	77.5	77.5	0.011	0.012	0.0073	1.5
M&F	LUAD	0.030	7.07	0.0101	177	165	77.5	85.0	0.051	0.051	0.0091	5.7
M&F	LUSC	0.030	7.69	0.0101	95.8	81.4	77.5	85.8	0.024	0.023	0.0092	2.6
M&F	MESO	0.030	10.2	0.0099	5.09	5.69	87.5	90.8	0.0014	0.0013	0.014	0.10
M&F	PAAD	0.026	7.02	0.0100	66.5	65.7	82.5	85.5	0.020	0.021	0.0095	2.2
M&F	PCPG	0.0032	4.11	0.0103	0.188	0.133	92.5	73.4	7.30E-05	6.00E-05	0.0065	0.011
M&F	READ	0.011	4.12	0.0087	37.0	35.8	82.5	87.5	0.016	0.019	0.013	1.2
M&F	SARC	0.014	6.06	0.0084	8.74	8.96	97.5	98.9	0.0029	0.0037	0.025	0.12
M&F	SKCM	0.021	5.67	0.0094	107	107	82.5	87.9	0.045	0.043	0.013	3.6
M&F	STAD	0.024	7.02	0.0096	43.3	46.5	87.5	89.5	0.016	0.015	0.013	1.3
M&F	THCA	0.0059	2.69	0.0101	28.6	26.4	67.5	62.4	0.016	0.016	0.0042	3.7
M&F	THYM	0.0094	5.54	0.0106	0.747	0.705	67.5	77.0	0.00026	0.00025	0.0061	0.043
M	Mean	0.0231	6.8	0.0100	42.3	45.8	82.5	85.0	0.015	0.015	0.014	1.06
M	SD	0.0092	1.7	0.0008	95.9	99.6	10.7	9.8	0.030	0.029	0.027	1.73
F	Mean	0.0174	5.9	0.0098	22.6	20.6	82.5	85.6	0.0078	0.0073	0.0075	0.97
F	SD	0.0084	1.5	0.0008	52.1	49.4	11.8	10.0	0.016	0.016	0.062	2.22
μ_M, μ_F^5	t test, P	0.000056	0.0033	0.034*	0.014†	0.012†	0.45	0.32	0.012†	0.0094†	0.035*	0.73

⁵The mean, SD and paired t -test P values in each column are for the 20 non-reproductive, paired cancer types for males and females, for the parameter in the corresponding column.

†Values are no longer significant to 5% level when Holm’s method for multiple-testing correction is applied for the paired t tests in the table

*Values are no longer significant to 10% level when Holm’s method for multiple-testing correction is applied for the paired t tests in the table.

Male (M) and female (F) parameter values from Table 1A, 1B are compared by paired t test for 20 paired cancer types in the last row of the table.

⁰Abbreviations for non-reproductive cancer types and footnotes 1-4 are explained in Table 1A. LGG and PCPG are cancer types with P values for model-fitted u_{μ} or k larger than 0.1 and were omitted from further analysis.

multiple comparison tests, which are described in the Supplementary Note 1. The term $(1 - bt)$ is zero when $t = b^{-1} = 98.2$ years for females and 94.1 years for males.

The mean b value for female reproductive cancers is 0.0117 ± 0.0008 (SD, $n = 5$, Table 1B, female). The b values of female reproductive cancers compared to the b values of their non-reproductive cancers (given above) are significantly different ($P = 0.002$), according to the Welch two-sample t test. This

assessment was not repeated for male reproductive cancers as only two cancer types were analyzed (Table 1A, male).

Stages, age of peak incidence, and stage-transition rate

We analyzed the trends in the number of cancer stages k , age of peak incidence (yr), and geometric mean of the stage-transition rate u_{μ} (yr⁻¹) of the

multistage-senescence model (Equation 5) with sex and different cancer types. There is a significantly greater (Welch two-sample non-paired t test, $P = 0.019$) mean number of stages of female non-reproductive cancers ($k = 5.9 \pm 1.5$ SD, $n = 20$) compared to their reproductive cancers ($k = 3.7 \pm 1.4$ SD, $n = 5$) (Table 1B, female).

The age of peak cancer incidence rate is dependent on the tumor suppression b and the number of stages k the cancer passes through until diagnosed; there is no dependence on geometric mean of the stage-transition rate u_{μ} . By taking the derivative of Equation 4, the age of peak incidence rate can be calculated (Equation 7), and consequently the model-fitted peak incidence rate (per 100,000 person-year). The age at peak incidence rate increases in a non-linear manner with k for male and female cancers (Figure 1A, 1B). There is an extremely significant Spearman's rank correlation with k for age at peak incidence rate, both model-fitted (both: Spearman's $\rho = 0.74$, $P = 0.0002$, $n = 21$; female: $\rho = 0.68$, $P = 0.0002$, $n = 25$; male: $\rho = 0.73$, $P = 0.0001$, $n = 23$) and from the SEER data (both: $\rho = 0.62$, $P = 0.003$, $n = 21$; female: $\rho = 0.66$, $P = 0.0003$, $n = 25$; male: $\rho = 0.47$, $P = 0.02$, $n = 23$).

The model-fitted cumulative probability of being diagnosed with at least one of the cancers considered is 41% for females and 55% for males, computed using Equation 8. These values are similar to 42% for females and 56% for males calculated from the SEER data directly.

There is an extremely significant linear relationship ($P < 0.0001$) of the geometric mean of the stage-transition rate u_{μ} with respect to the number of stages k , (Figure 2A, 2B). Given the assumption that stages occur at the same rate, Figure 2A, 2B indicate that the rate of change of each stage is faster when there are more stages in a cancer. However, if the assumption does not hold, one possibility that would be consistent with this pattern is that rates are slower during the initial stages of cancer initiation and increase during later stages (see Discussion). The linear regression analyzes of the geometric mean of the stage-transition rate u_{μ} versus the number of stages k , were compared for males and females by one-way analysis of variance, ANOVA and the slopes and intercepts did not differ significantly between paired regions (Supplementary Note 2).

There is an extremely significant variation in u_{μ} for non-reproductive cancers between sexes, according to the paired t test, with the u_{μ} value for male cancers on average about one-third greater than that for females for the same cancer ($n = 20$, $P < 0.0001$).

Two-variable model

In previous publications on the multistage and multistage-senescence models, only the trends in cancer incidence rate were analyzed, whereas we developed a two-variable model (age and the number of carcinogenic stages) that uniquely takes account of the relative magnitude of incidence rate of different cancers.

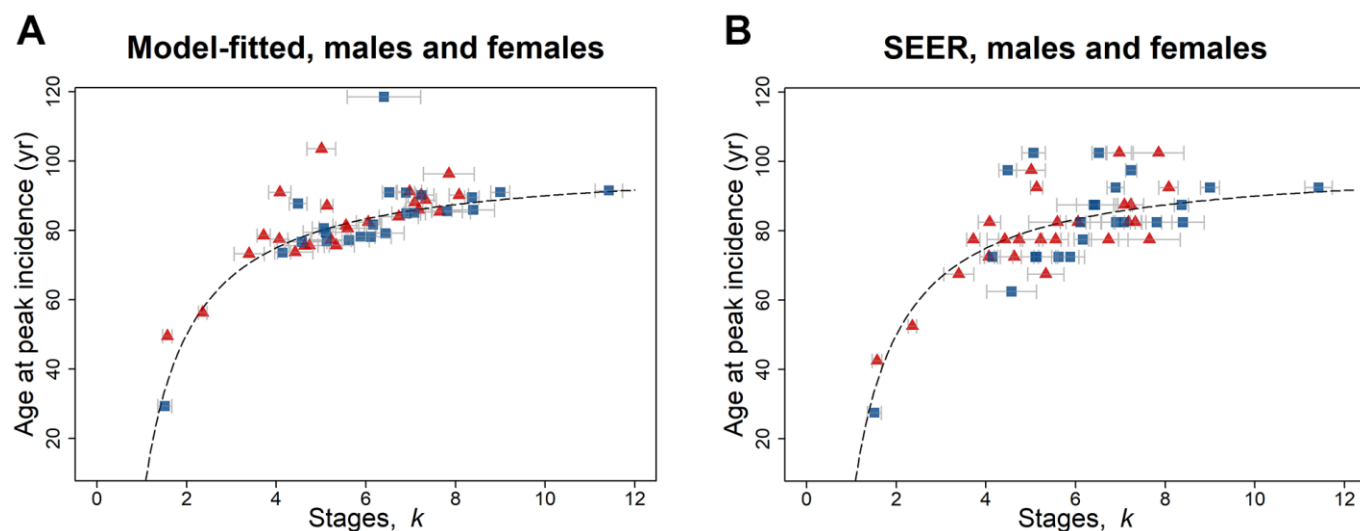


Figure 1. Age at peak incidence (years) versus number of stages k for SEER data for 2010–2013, for males (blue squares) and females (red triangles) and for both reproductive and non-reproductive cancers (Table 1A, 1B). Both (A) model-fitted and (B) SEER age at peak incidence have a highly significant positive association with k . The dashed line indicates the peak incidence age given by Equation 7 with $b = 0.01$. The gray bars indicate one standard error in the estimate of k .

An age- and stage-dependent model is obtained by substituting in Equation 5 for u :

$$ASR(t) = (c \cdot k - d)^k / \Gamma(k) \cdot t^{k-1} \cdot (1 - bt) \quad (6)$$

where constants b , c , and d equal 0.0099, 0.0046, and 0.0087, respectively, as assessed for non-reproductive cancers of both sexes pooled (Figure 3). The effects of the senescence tumor suppressor factor employing the

two-variable model are considerable as assessed from the increase in cumulative probability of cancer over a lifetime and the change in b value from 0.0099 (mean of non-reproductive cancers for both sexes pooled) to zero. For cancer stages $k = 2, 3, 4, 6,$ and 8 , the cumulative probability up to 101 years ($=1/b$) was reduced by 67, 75, 80, 85, and 88%, respectively (Supplementary Note 3), indicating greater tumor suppression b for the more complex cancers of longer latent periods. The age of

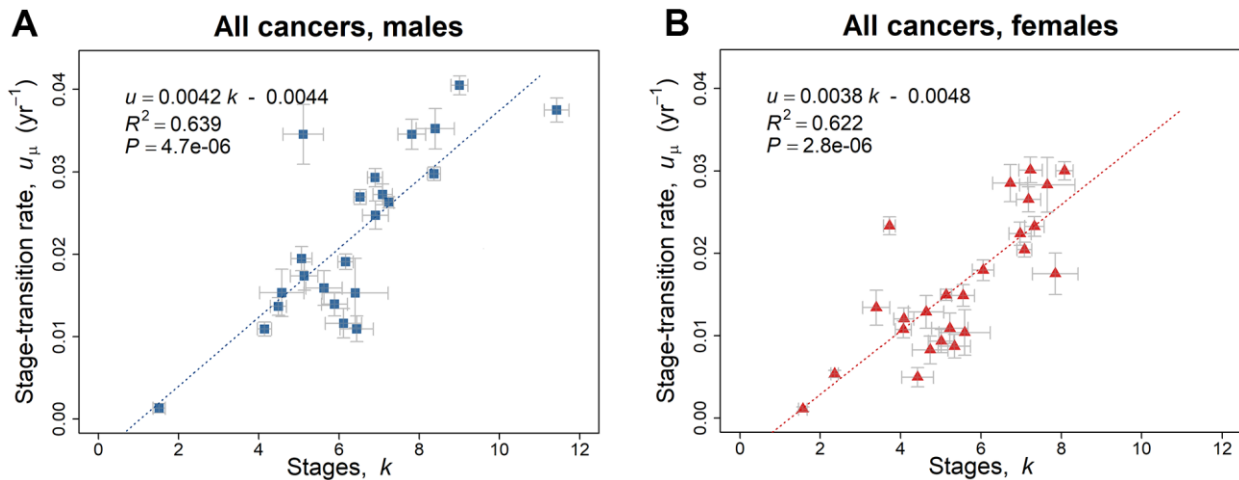


Figure 2. Linear regression trend line of the geometric mean of the stage-transition rate u_μ versus the number of stages k , employing the 2010–2013 SEER data based on the model of Equation 5. (A) Blue squares represent values for males (Table 1A). (B) Red triangles represent values for females (Table 1B). The gray bars indicate one standard error in the estimate of the parameters by non-linear least squares.

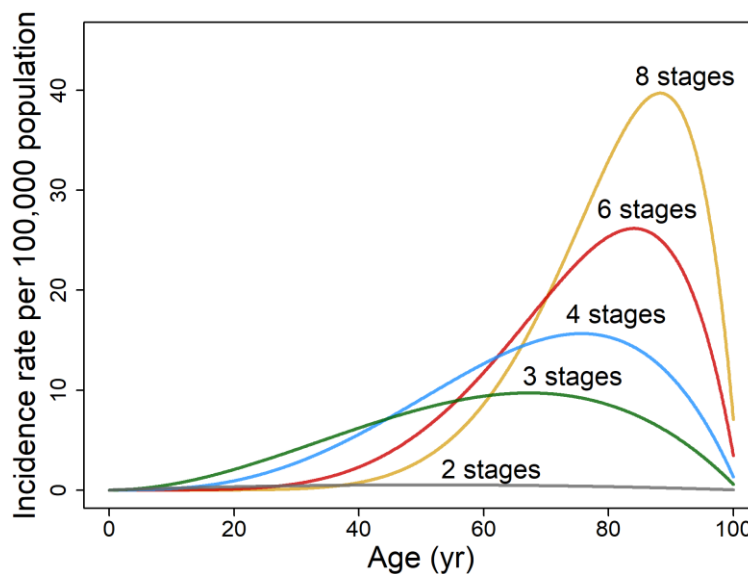


Figure 3. Illustrative plots of age-specific rate of cancer incidence per 100,000 population based on two variables, age t and cancer stages k . The age-dependent incidence rate of hypothetical cancers is modeled on non-reproductive cancers for both sexes pooled ($n = 21$) as described by Equation 6 (assuming $b = 0.0099$, $c = 0.0046$ and $d = 0.0087$).

(standardized residual ≥ 3.0), was excluded from the analysis as it was the only type of cancer that demonstrated more driver genes than the number of stages. Endometrial cancers consist of four categories with highly variable mutation frequency and copy number [15]. Driver mutations from Iranzo et al. [14] are linearly correlated to a moderate degree with the number of stages in the 2010–2013 data (Pearson's $r = 0.42$, $P = 0.033$, $n = 26$) and in the 2000–2003 data (Pearson's $r = 0.39$, $P = 0.054$, $n = 25$). In terms of percentage contribution from driver mutations to the number of stages, the mean is 34% (similar in value to that derived from Table 2) with a wide 95% confidence interval of 9.9% and 64.3%, possibly partly due to differing contributions of driver genes to carcinogenesis as detailed in the Discussion. Comparing the number of stages with the number of driver genes from Bailey et al. [16] yields a weak correlation (Pearson's $r = 0.31$, $P = 0.12$, $n = 26$ from 2010–2013 data; Pearson's $r = 0.30$, $P = 0.15$, $n = 25$, from 2000–2003 data).

DISCUSSION

This analysis shows that the synchrony in both the rise and fall of U.S. SEER cancer incidence in aging adults is profound, with the possible evolution of the stage-transition rate and senescence tumor suppression mechanisms. However, the task of disentangling and quantitatively identifying aging effects on cancer etiology is recognized to be especially difficult, with on the one hand effects that promote cancer such as inflammation and genomic instability [17] and on the other hand senescence-related defensive systems that suppress cancer.

Senescence tumor suppression

The tumor suppression factor b (yr^{-1}) is relatively constant for non-reproductive cancers regardless of cancer type or sex. Senescence tumor suppression is assumed to increase linearly with age. There are various potential cellular mechanisms that likely contribute to the suppression of malignant cancers in old age such as telomere erosion, Hayflick limit, stem cell exhaustion, senescent cells, accelerating systemic mass loss, and epigenetic aging changes [18–20]. For example, apoptosis rates in bone marrow increased from ~7% of cells, both in 0- to 9-year-olds and in 50- to 59-year-olds, rising to three-fold more in 80- to 100-year-olds [21]. The tumor suppressor factor is of a similar value whether the malignancy is mesothelioma primary arising from inhaled asbestos, cervical cancer from exposure to human papillomavirus, melanomas from sun exposure, or post-menopausal breast cancer with elevated insulin levels. The constancy of the tumor suppression factor indicates tissue adaptation to

various extrinsic environmental causes of cancer. The suppression of malignant tumors is accompanied by an increase in the prevalence of benign cancers. Imaida et al. [22] studied autopsies of 871 Japanese patients aged 48 to 113 years at death and found that the ratio of prevalence of latent cancers (those not diagnosed clinically) to cancers with metastasis increases from 0.64 in 48- to 84-year-old patients to 1.4 in older patients. Although there is evidence of mosaic aging of normal tissues [23], overwhelmingly there is synchrony in systemic aging [24] and the tumor suppressor factor, which is accompanied by the decline of cancer incidence rates for all cancer types in the aging adult.

The aggregated SEER cumulative probability over lifespan of 20 non-reproductive cancers analyzed is 73% greater for males than for females (Table 1C). In parallel with this, males have a greater acceleration of mass loss than females as measured in some major organs and body cell mass of normal populations [24]. This may be indicative of a greater rate of aging in males [25]. DNA mutation accumulation is greater in sex-specific cancers [26]. The tumor suppression of female reproductive cancers is shown to be stronger than for female non-reproductive cancers. A possible tumor suppressive mechanism is the early onset of mass loss in female reproductive organs compared to non-reproductive ones (breast, ovary, and uterus at about 25, 35, and 21 years of age, respectively) and an elevated decline in mass loss of functional tissue (breast, ovary, and uterus lose about 35, 46, and 35% mass, respectively, from 25 to 70 years of age) [24]. This greater suppression of female reproductive cancers may be an evolutionary adaptation to counter estrogen having a strong proliferative effect.

The interplay between the p53 master tumor suppressor and insulin-like growth factor 1 (IGF-1), which stimulates the mammalian target of rapamycin (mTOR), is critical to normal cell growth and carcinogenesis: viable p53 down-regulates these two highly evolutionary-conserved pathways [27]. In fact, insulin, growth factors and amino acids all activate the mTOR pathway, which stimulates protein synthesis and cell growth [25]. IGF-1 production provides an important protein determining post-natal growth and growth hormone (GH) signaling. Adversely, IGF-1 is not directly mutagenic but a potent mitogen and cancer risk; for example, prospective blood samples show elevated IGF-1 levels in individuals later diagnosed with prostate and pancreatic cancer [28, 29]. IGF-1 has also been implicated in increased cancer risk of breast, colorectal, lung, and other cancers [30]. The down-regulation of the GH/IGF-1/insulin system decreases cancer risk and increases longevity in animal models; however, in

Table 2. The number of driver genes and mutations as assessed by Iranzo et al. [14] and Bailey et al. [16], compared to the number of stages as given for both sexes of SEER incidence data pooled (Table 1C), except for reproductive cancers (Table 1A, 1B).

TCGA	Driver genes mutations (Iranzo et al.)	Driver genes mutations (Bailey et al.)	SEER <i>k</i> stages	Non-driver gene stages (Iranzo et al.)	Non-driver gene stages (Bailey et al.)
ACC	1.61	0.52	5.10	3.48	4.58
BLCA	3.09	5.10	8.47	5.38	3.37
BRCA	1.62	1.84	3.72	2.10	1.88
CESC	1.02	1.89	1.57	0.55	-0.32
COADREAD	3.24	3.84	6.32	3.09	2.48
ESCA	1.72	1.87	6.64	4.92	4.77
GBM	1.51	1.84	5.65	4.15	3.81
HNSC	2.27	3.21	4.87	2.59	1.66
KICH	0.64	0.48	5.17	4.53	4.69
KIRC	1.63	1.45	4.69	3.06	3.24
KIRP	1.14	0.35	5.05	3.91	4.70
LAML	2.13	0.77	7.77	5.64	7.00
LIHC	1.38	1.84	4.69	3.30	2.85
LUAD	1.95	2.19	7.07	5.12	4.88
LUSC	2.19	2.68	7.69	5.50	5.01
MESO	1.24	0.87	10.2	8.97	9.33
OV	1.31	1.19	4.07	2.76	2.88
PAAD	2.44	2.19	7.02	4.58	4.83
PRAD	0.84	0.55	5.11	4.27	4.56
SARC	1.26	0.63	6.06	4.79	5.43
SKCM	2.15	2.45	5.67	3.52	3.22
STAD	1.05	1.92	7.02	5.97	5.10
TGCT	1.19	0.34	1.52	0.33	1.18
THCA	1.06	0.77	2.69	1.64	1.92
THYM	1.10	0.63	5.54	4.44	4.91
UCEC	3.71	7.34	3.40	-0.31	-3.94
UCS	2.51	3.13	5.59	3.09	2.46
Average [including UCEC]	[1.74]	[1.92]	[5.49]	[3.75]	[3.57]
Average excluding UCEC	1.67	1.71	5.58	3.91	3.86
Average (non-reproductive only)	1.74	1.78	6.17	4.43	4.39

humans the results are somewhat contradictory, although genetic studies of the GH/IGF-1/insulin system support their involvement in human longevity [31]. Cancer is virtually unknown in patients with congenital IGF-1 deficiency, exhibiting dwarfism and obesity [32]. A meta-analysis study confirms that the prevalence of most cancers increases with adult height, which is influenced by hormone levels, especially growth factors [33]. Multiple studies of serum IGF-1 concentrations show an increase in adolescence, a peak during puberty, and then initially in adulthood a rapid decline; thereafter IGF-1 levels change more slowly to about a fifth to a tenth of the maximal value at 80 years of age [34, 35]. For both sexes, the multicenter and largest study [36] measured the annual fractional decline in IGF-1 activity (estimated

as the gradient over the intercept of a linear trend between 25 and 80 years) of about 0.0087, which is similar to the tumor suppressor factor *b* value of 0.0099. Growth hormones can have a profound influence on both normal and carcinogenic tissues. Organ functional mass loss, greater than fat-free mass loss, starting early in adulthood and accelerating in old age may be indicative of the reduction in primary growth hormones and metabolic rate with adult age [24, 37]. Consequently, the systemic cancer suppressor factor *b* and involuntional changes could therefore be associated with the declining plasma IGF-1 in aging adults.

Cancer and aging are inextricably interconnected. In 1957, Williams [38] proposed the theory of antagonistic

pleiotropy: genes such as *TP53* or transforming growth factor- β (*TGF- β*), and biological processes that enhance reproductive success early in life, lead to an evolutionary trade-off, with later fitness decline and death. In this view, p53-dependent replicative senescence would be one such biological process. In terms of cancer, p53, replicative senescence, and indeed growth hormones are a double-edged mechanism: they can both advance and impede oncogenesis [39, 40]. Contemporary observations are that longevity-enhancing, protective, genetic variants become more prevalent with increasing age of the very old [41]. The heritability of living to the mid-80s is only 20–30% (twin study [42]); however, the heritability of living past 100 is between 33% (females) and 48% (males). Hence, there is the possibility that the evolution of tumor suppression, although associated with frailty, nevertheless counteracts cancer in the very old.

Stages

This work demonstrates that adult cancers with an early age of peak incidence rate (yr) have fewer cancer stages k than more complex cancers that reach maximum incidence rate at a later age (Figure 1A, 1B). The multistage model is based on cellular changes that are specific, discrete, and stable and that proceed in a unique order, although the changes are not necessarily gene mutations [7, 43]. Malignant tumors typically acquire a range of biological capabilities or hallmarks that include proliferating in a sustained manner, evading growth suppression, resisting cell death, acquiring replicative immortality, inducing angiogenesis, and activating invasion and metastasis [17]. Biological mechanisms that support these hallmarks include genetic mutations and epigenetic modifications [5, 44]. Most cancer cell lines also exhibit very short telomeres but escape replicative senescence through mechanisms such as telomerase activation or telomeric recombination [45–47]. Four-fifths of tumors are solid tumors, which generate a blood vascular supply to supply nutrients and oxygen to enable growth beyond a few millimeters. Two-thirds of solid tumours in a Norwegian population registered with metastases at death [48]. This process involves genetic and epigenetic changes in which cells commonly change their phenotype such as during epithelial-to-mesenchymal transition or mesenchymal-to-epithelial transition and exhibit hybrid features via intermediate or partial states [49, 50].

Stage-transition rate

The geometric mean of the stage-transition rate u_{μ} (yr^{-1}) has a wide range from 0.00064 to 0.040 for the various cancer types (Table 1A–1C) and its increase with the number of stages k is remarkably robust (Figure 2A,

2B). For example, testicular cancer, TGCT with 1.5 stages has a value of u_{μ} of 0.0013, whereas for bladder cancer, BLCA with 8.5 stages, u_{μ} is 0.036 for both sexes pooled. Therefore, if the number of cancer stages is small, the duration of each stage is longer. This finding may result from earlier stages being of longer duration than later ones. One could speculate that if, contrary to our findings, the transition rate was initially rapid, then the cumulative incidence of the cancer could be extremely high by middle age, so there would be strong evolutionary pressures to reduce the incidence of the cancer. This pressure could result in addition obstacles to the cancer's formation, which would then require additional mutations for a cancer to overcome. In this way, a fewer-stage cancer could be converted to a many-stage cancer. Therefore, it appears that cancer cells out-compete aging, slower-dividing, normal cells by acquiring quickening carcinogenic stages via Darwinian selection that widens the cancer cell traits from those of the initial cell, and in the process augments the competitive advantages of cancer cells (especially high-stage tumors) over those of the surrounding non-cancer cells [51].

Several tumor suppression factors have been posited as influencing the generally lower cancer rates in women than men, including adult females having generally shorter stature, longer telomeres, less telomere attrition and lower rates of thymic involution, healthier lifestyles, better T cell production, and more robust p53 response [52–54]. An exception is DNA methylation, which is the most accurate parameter of biological aging and a tumor suppression factor that has equal influence in men and women [20]. We identified some additional gender-specific carcinogenic factors by comparing the parameters of the multistage-senescence model derived for 20 types of non-reproductive cancers in males and females (Table 1C). For example, cancers in males have ~14% more stages than those in females ($P = 0.0033$). Intriguingly, the geometric mean of the stage-transition rate u_{μ} in males is 33% greater than that of females ($P < 0.0001$). This is a novel explanation of male susceptibility to carcinogenesis. However, it is worth further consideration because a small change in the stage-transition rate u results in a large change in the incidence rate, as u is raised to the power k . Surprisingly, there is no sex-dependent significant difference in the extrinsic-risk-dependent parameter, the SEER to two-variable model ratio of the cumulative probability over a lifetime, which tentatively infers that male susceptibility is not due to lifestyle.

Two-variable model

Although the two-variable model based on age- and stage-dependence is too broad a stroke to characterize

cancer incidence for all cancer types, it is instructive to analyze the trends it describes. The two-variable model for non-reproductive cancers indicates that for a small number of stages, the peak incidence rate is lower and occurs at a younger age (Figure 3). Complex cancers, compared to those with few stages, have a much higher cumulative incidence; for example, the cumulative probability over lifespan of an eight-stage cancer is 33 times that of a rarer two-stage cancer. Therefore, in general, the more complex the staging of specific adult cancers, the higher the cancer incidence rates and the longer the latent periods. Another observation is that the early age of peak incidence rates of cancers with fewer stages have far broader incidence rate peaks than the more complex cancers, somewhat due to lesser influence of senescence earlier in adulthood. Age 60 years appears pivotal; before that age cancers with few stages dominate diagnoses, whereas after that age high-stage cancers dominate incidence rates.

There is great variation in the endogenous (e.g., biologic aging) and exogenous (i.e., radiation) non-intrinsic factors driving the total cancer risk and the age-adjusted incidence rate of regions around the world, with the ratio of high to low incidence rates being up to ten-fold or more [13]. A finding was that the two-variable, age- and stage-dependent model is highly dependent on the intrinsic risk of carcinogenesis [13]. This was determined by the strong association ($P = 0.005$) of the ratio of the cumulative probability of cancer over lifespan, calculated from SEER data (numerator) and the two-variable model (denominator), with the ratio of the extrinsic cancer risk (numerator) and the intrinsic cancer risk (denominator). Hence, there appears to be an evolutionary component to multistage [55] and multistage-senescence models, where natural selection acts to suppress early-onset, rare, low-stage cancers when able to effect Darwinian fitness, which is less effective as reproductive rates decline and late-onset, common, high-stage cancers develop.

Driver mutations

All cancers possess somatically acquired mutations. Most somatic mutations are passenger mutations, which far outnumber, and rise with, the number of mutational driver genes [14]. Sporadic cancers arise through somatic evolution that parallels the increase in mutations in normal cells with aging. Early events in a cancer's development are characterized by a constrained set of common driver genes, and later events are ascribed to a greater set (~four-fold more) of drivers and increased genomic instability [56]. This applies to different cancer types and subtypes. Primary tumor cells may lie dormant for years before circulating cells form metastases [50]. Only ~0.03% of circulating melanoma

cells in mice formed lung metastases [57]. However, other researchers report that the formation of driver gene mutations mainly arises during the initial stages of carcinogenesis, as primary and metastatic tumors share almost the same driver genes [58]. Non-shared metastatic driver genes do not have functional consequences. The median number of mutated driver genes was three for adult acute myeloid leukaemia, with the number of driver mutations increasing with age [59]. The mean number of driver gene mutations of various cancer types is approximately two (Table 2), [14, 16].

Mutations in the *TP53* gene (or p53 protein), the most common driver gene in cancers, particularly epithelial cancers, significantly increase in tumors with a high number of stages as evaluated from the steepness of the power function rise in cancer rates with aging (Equation 1) [60]. Driver gene mutations can contribute to one or more stages. This quantitative trend of the loss of the *TP53* gene increasing with a cancer's stages can be interpreted as p53 contributing to multiple carcinogenic stages and promoting increasingly rapid progression. Early mutations dominate cancerous tissues, as shown in breast cancer [61]. This is supportive of metastatic driver genes arising early in the cancer development, (especially those involving oncogenes *TP53* and *KRAS*) [62], although further stages comprise the metastatic process. Notwithstanding the central dogma in oncology of the dominant role of driver genes and mutations, by our analysis driver mutations contribute (making no allowance for non-singular driver mutations contributions) to only approximately one-third of the carcinogenic stages, which underlines the complexity of tumorigenesis [63].

Models of carcinogenesis

There are many alternatives to the multistage-senescence model of carcinogenesis. A review of carcinogenic models identified five mathematical model types, namely mutations, genomic instability, non-genotoxic mechanisms, Darwinian cell selection, and tissue organization [29]. A well-known model by Moolgavkar, Venzon, and Knudson (MVK) [64], based on a two-mutation initiation-promotion process, seeks to address a considered deficiency of the Armitage–Doll model [7] in that it takes account of cell division and differentiation. This model is especially suited to childhood cancers such as the most common type, acute lymphoblastic leukemia, and the much rarer tumor, retinoblastoma, which have been experimentally and theoretically shown to have undergone two genetic changes [65, 66]. Childhood cancers often result from defects in developmental signaling pathways of stem cells [19, 67]. Obviously, the primary incidence peak of

childhood cancers is not influenced by senescence as represented by the multistage-senescence model. However, cancer models have been produced based on genomic instability and the somatic cellular evolution of cancer likely common to tumors of all ages [68]; notwithstanding, childhood and adult cancer develop and require models of a different nature.

The decline in cancer incidence rates in old age has been modeled by Cook et al. [69] for stomach cancer in males assuming that only 1% of the population is susceptible to this cancer; the modeling led to similar fits between the susceptibility and multistage-senescence models except for those aged more than 105 years. Our model is in agreement with the analysis of Cook et al. [69], indicating incidence peaks at a younger age for rarer cancers. However, Ritter et al. [70] suggest that it is unlikely that cancer-susceptible people are depleted after age 80. A recent analysis by Belikov [71] shows that Erlang probability distributions (summing independent, exponentially-distributed events or stages) closely follow U.S. SEER incidence rate curves for 20 prevalent cancers. No account is taken of a cellular-senescence component being a factor in cancer downturn in old age. The analysis generates the number of successive, carcinogenic events, with a very wide and perhaps improbably large range of 4 to 41 stages, proffered to be driver mutations or epimutations. Based particularly on colorectal cancer common in adulthood, it has been proposed that three driver genes are needed for a cell to evolve through breakthrough, expansion, and invasive stages to an advanced cancer [72]. Whereas our study estimates the number of stages for colorectal cancer, COADREAD (Table 1A–1C) as between six and seven stages, maybe including observed epigenetic modifications [5, 44]. The Armitage–Doll and MVM models both assumed a constancy in the number of stages for all tumor types, although analysis of contemporary SEER and driver gene data and contemporary understanding of the development of genomic instability, epigenetic changes, and metastases indicate that this is certainly not the case.

Limitations of determining temporal trends in cancer incidence

Finally, there is a limited potential to identify temporal trends in multistage-senescence model parameter values as seen in the five data sets consisting of the 1979–1983, 1989–1993, and 1999–2003 data from Harding et al. [9], and the corresponding 2000–2003 and 2010–2013 data from Supplementary Tables 5A–5C, 4A–4C, respectively. For example, a fall in the number of stages of prostate cancers from ten to about five was a trend evident in the SEER data sets from 1979–1983 to 2010–2013 (Supplementary Figure 1). Care was taken to

duplicate the data retrieval and fitting methods of Harding et al. [9], as three of the five data sets originate from this published study. Of course, ideally all data sets used would derive from our labors, although data from the 2000–2003 and 2010–2013 groups come from a larger geographic region than those of earlier years. There is an overlap in the 1999–2003 and 2000–2003 data sets, with four independent data sets, not five, which limits temporal analyzes.

The prostate cancer incidence rate is influenced by its detection by transurethral resection of the prostate and by prostate-specific antigen (PSA) [73]. The use of PSA tests from 1986 onwards in the U.S. has allowed the early detection of prostate cancer. This has also resulted in considerable overdiagnosis because detection of prostate cancer would otherwise not have been diagnosed within the patient’s lifetime. An Australian study indicated that overdiagnosis was common in prostate, breast, renal, and thyroid cancers, and melanoma [74]. An analysis of SEER data from 1988 to 1998 indicated over-diagnosed prostate cancer rates of ~29% for white subjects and 44% for black subjects [73]. It is proposed that early- and over-diagnosis due to PSA availability may partly explain the declining number of stages in prostate cancers diagnosed over four decades. This demonstrates the potential to examine temporal trends in incidence-related parameters, provided there is future analysis of more data sets.

A generalized limitation of our analyzes of age-specific rate of cancer incidence is their cross-sectional nature. The age-specific incidences rates emanate from various groups of people, who may have different cancer risks for reasons other than age itself, and these reasons are not accounted for in the carcinogenesis models. Hanson et al. [75] point out that cross-sectional cancer incidence studies often offer limited conclusions about cancer trends due to aggregated ages above 85 years or the examination of a single period or fail to consider period and cohort influences — only the last of these is a limitation of our study. There are significant differences between the characteristics of the TCGA and SEER datasets, such as age and stage at diagnosis [76]. The potential inaccuracy of population estimates for age groups above 85 years was investigated in a data quality study by Miller et al. [77] that analyzed (in a similar manner to our study) the 2010 Census and U.S. SEER registry records for 2008–2012, which yielded cancer incidence rates that usually did peak (a trend observed in our study) and then decrease in the oldest old.

CONCLUSION

A multitude of carcinogenic models have been proposed in the scientific literature; however, the multistage-

senescence model is unique in quantifying several important parameters of the age-specific incidence rate of different cancer types based solely on the number of development stages. The finding, perhaps controversial, that cancer-suppressive mechanisms counter the aging-dependent escalation in cancer complexity and incidence gives support to preventing cancer by augmenting extant mechanisms. The two-variable model gives us a useful tool to further investigate the biological mechanisms that drive specific cancers, such as those that are affected by ethnicity or ionizing radiation.

MATERIALS AND METHODS

All statistical analysis was performed using software R version 3.6.0 [78]. The full code for all analyzes (including processing data, computing incidence rates, statistical analysis, and making plots) that we developed at the time of publication, under MIT License, for estimating cancer incidence rates is posted in the GitHub repository at <https://github.com/canghel/cancer-incidence-v5>.

SEER cancer incidence data

The methods to estimate incidence rates from person-years at risk for the older U.S population and to fit the multistage-senescence model were reproduced as closely as possible from Harding et al. [9]. The age-specific rate of cancer incidence data from the SEER cancer registry were analyzed were for 2000–2003 and 2010–2013. This was to allow use of the SEER 18 registries data for all the calculations [10], to be near in date to the Census 2000 and 2010 population estimates [12], and to allow reasonable comparison to previous literature. As in Harding et al. [9], we restricted the selection of cases to malignant behavior, known age, and first matching record for each person.

The incidence cases of 30 cancer types corresponding to TCGA cancer types [76] were extracted from the SEER data [10] using SEER*Stat 8.3.5 software. The cancer types consist of 23 non-reproductive cancers as well as five female-specific cancers and two male-specific cancers. The TCGA codes and SEER histology correspondence are given in Supplementary Table 3 [76]. The number of cancer cases of each type, sex, and age-range was downloaded separately for each of the 18 SEER registries.

For ages up to 85 years the SEER-provided population estimates were used. The U.S. Census 2000 and 2010 populations [12] for each registry agree well with the 2000 and 2010 corresponding SEER populations for all registries except for the Alaska Native Tumor Registry. For ages 85 and greater we calculated the

fraction of the 85+ population by sex in each registry and in each of the age groups 85–89, 90–94, 100–104, 105–109, and 110+ using the U.S. Census data for 2000 and 2010. We used the Census population older ages fractions to infer the populations for the oldest categories, assuming that these fractions remain constant over the subsequent three years. The discrepancy between such ratios is less than ~15% for the groups under 85 years.

The crude rate per 100,000 persons in each five-year age category were determined and the associated standard error. Although the assumption of constant 85+ population fractions over time may fail for the oldest populations, especially for males with higher mortality rates, the computed standard errors for the incidence rates in these populations are also large and hence these incidence rates to the multistage beta model fit. For the peak age of incidence and the peak rate of incidence, we restricted the values reported to ages less than 105 to avoid outliers.

Multistage-senescence model fit

We fit the multistage-senescence model (Equation 4) by non-linear least squares, weighted proportionally to the inverse standard error squared, using the Levenberg–Marquardt algorithm from the `minpack.lm` v.1.2-1 package [79] in R v.3.6.0 [78]. The curves were fit beginning at age 50 when the number of cases for each cancer begins to rise [9], with three exceptions where the incidence peaks at much younger ages than most cancer types: thyroid carcinoma (THCA) and cervical squamous cell carcinoma and endocervical adenocarcinoma (CESC) both for females at 30 years, and testicular germ cell tumors (TGCT) in males at 20 years. The time t in Equations 4 and 5 corresponds to age in non-reproductive cancers and to time since the onset of puberty, estimated as age minus 15 years in reproductive cancers.

By taking the derivative of Equation 4 [80], the age of peak incidence is

$$T_p(k) = k / (b \cdot (k + 1)) \quad (7)$$

The total probability of each cancer type, the cumulative ASR, computed analogously for Equation 4 as in Pompei and Wilson [80] is

$$P_c = \int_0^{1/b} ASR(t)dt = \int_0^{1/b} at^{k-1}(1-bt)dt \quad (8)$$

$$= \frac{a}{b^k} \left(\frac{1}{k} - \frac{1}{k+1} \right) = \frac{a^k}{\Gamma(k)} \frac{1}{b^k} \left(\frac{1}{k} - \frac{1}{k+1} \right)$$

Parameter a is a multiplicative term [7], whose values are given in Supplementary Tables 4A–4C, 5A–5C.

TCGA driver gene data

The number of driver mutations are taken from Table S6, of Iranzo, Martincorena [14], with the total number of samples per cancer type assumed to be the same as in Martincorena, Raine [81].

Additional information

Supplementary information is available in the online version of the paper. The full code and additional documentation at the time of publication, under MIT License, is posted in the GitHub repository at <https://github.com/canghel/cancer-incidence-v5>.

AUTHOR CONTRIBUTIONS

R.B.R. designed the study, carried out exploratory analysis based on published data, and wrote the first version of the paper. C.V.A. carried out data processing and computational analysis. D.S.D. carried out data processing and computational analysis and provided statistical expertise. All authors participated in the interpretation of the results, critically revised the paper, and approved the final version to be published.

ACKNOWLEDGMENTS

This study has benefited from the library facilities that McGill University makes available to its adjunct professors (R.B.R.). We are very grateful to Helena Rummens of Deep River, Ontario for assistance in editing the paper. An anonymous reviewer is thanked for critically reading the manuscript and suggesting thoughtful improvements.

CONFLICTS OF INTEREST

The authors declare that they have no conflicts of interest.

FUNDING

This work was supported by the Federal Nuclear Science and Technology Work Plan of Atomic Energy of Canada Limited.

REFERENCES

1. Pavlidis N, Stanta G, Audisio RA. Cancer prevalence and mortality in centenarians: a systematic review. *Crit Rev Oncol Hematol*. 2012; 83:145–52. <https://doi.org/10.1016/j.critrevonc.2011.09.007> PMID:22024388
2. Frank SA. A multistage theory of age-specific acceleration in human mortality. *BMC Biol*. 2004; 2:16. <https://doi.org/10.1186/1741-7007-2-16> PMID:15242520
3. Cho H, Mariotto AB, Schwartz LM, Luo J, Woloshin S. When do changes in cancer survival mean progress? The insight from population incidence and mortality. *J Natl Cancer Inst Monogr*. 2014; 2014:187–97. <https://doi.org/10.1093/jncimonographs/lgu014> PMID:25417232
4. Fisher JC, Hollomon JH. A hypothesis for the origin of cancer foci. *Cancer*. 1951; 4:916–18. [https://doi.org/10.1002/1097-0142\(195109\)4:5<916::aid-cnrc2820040504>3.0.co;2-7](https://doi.org/10.1002/1097-0142(195109)4:5<916::aid-cnrc2820040504>3.0.co;2-7) PMID:14879355
5. Frank SA. *Dynamics of Cancer: Incidence, Inheritance, and Evolution*. Princeton (NJ): Princeton University Press; 2007. PMID:20821846
6. Nordling CO. A new theory on cancer-inducing mechanism. *Br J Cancer*. 1953; 7:68–72. <https://doi.org/10.1038/bjc.1953.8> PMID:13051507
7. Armitage P, Doll R. The age distribution of cancer and a multi-stage theory of carcinogenesis. *Br J Cancer*. 1954; 8:1–12. <https://doi.org/10.1038/bjc.1954.1> PMID:13172380
8. Pompei F, Wilson R. Age distribution of cancer: The incidence turnover at old age. *Hum Ecol Risk Assess*. 2001; 7:1619–50. <https://doi.org/10.1080/20018091095267>
9. Harding C, Pompei F, Lee EE, Wilson R. Cancer suppression at old age. *Cancer Res*. 2008; 68:4465–78. <https://doi.org/10.1158/0008-5472.CAN-07-1670> PMID:18519710
10. Surveillance, Epidemiology, and End Results (SEER) Program. Bethesda (MD): National Cancer Institute. SEER*Stat Database: Incidence - SEER 18 Regs Research Data + Hurricane Katrina Impacted Louisiana Cases, Nov 2017 Sub (2000-2015) <Katrina/Rita Population Adjustment> - Linked To County Attributes - Total U.S., 1969-2016 Counties, National Cancer Institute, DCCPS, Surveillance Research Program, released April 2018, based on the November 2017 submission. Age recode with <1 year olds. 2018. <http://seer.cancer.gov/seerstat/>
11. Ries LAG, Eisner MP, Kosary CL, Hankey B, Miller B, Clegg L, Edwards BK. *SEER Cancer Statistics Review, 1973-1997*. (Bethesda, MD, USA: National Cancer Institute). 2000. https://seer.cancer.gov/archive/csr/1973_1997/
12. US Census Bureau. 2010 Census Special Reports C,

- C2010SR-03. Washington, DC: US Government Printing Office. 2012. <https://www.census.gov/prod/cen2010/reports/c2010sr-03.pdf>
13. Wu S, Powers S, Zhu W, Hannun YA. Substantial contribution of extrinsic risk factors to cancer development. *Nature*. 2016; 529:43–47. <https://doi.org/10.1038/nature16166> PMID:[26675728](https://pubmed.ncbi.nlm.nih.gov/26675728/)
 14. Iranzo J, Martincorena I, Koonin EV. Cancer-mutation network and the number and specificity of driver mutations. *Proc Natl Acad Sci USA*. 2018; 115:E6010–19. <https://doi.org/10.1073/pnas.1803155115> PMID:[29895694](https://pubmed.ncbi.nlm.nih.gov/29895694/)
 15. Kandoth C, Schultz N, Cherniack AD, Akbani R, Liu Y, Shen H, Robertson AG, Pashtan I, Shen R, Benz CC, Yau C, Laird PW, Ding L, et al, and Cancer Genome Atlas Research Network. Integrated genomic characterization of endometrial carcinoma. *Nature*. 2013; 497:67–73. <https://doi.org/10.1038/nature12113> PMID:[23636398](https://pubmed.ncbi.nlm.nih.gov/23636398/)
 16. Bailey MH, Tokheim C, Porta-Pardo E, Sengupta S, Bertrand D, Weerasinghe A, Colaprico A, Wendl MC, Kim J, Reardon B, Ng PK, Jeong KJ, Cao S, et al, and MC3 Working Group, and Cancer Genome Atlas Research Network. Comprehensive characterization of cancer driver genes and mutations. *Cell*. 2018; 173:371–85.e18. <https://doi.org/10.1016/j.cell.2018.02.060> PMID:[29625053](https://pubmed.ncbi.nlm.nih.gov/29625053/)
 17. Hanahan D, Weinberg RA. Hallmarks of cancer: the next generation. *Cell*. 2011; 144:646–74. <https://doi.org/10.1016/j.cell.2011.02.013> PMID:[21376230](https://pubmed.ncbi.nlm.nih.gov/21376230/)
 18. Hayflick L, Moorhead PS. The serial cultivation of human diploid cell strains. *Exp Cell Res*. 1961; 25:585–621. [https://doi.org/10.1016/0014-4827\(61\)90192-6](https://doi.org/10.1016/0014-4827(61)90192-6) PMID:[13905658](https://pubmed.ncbi.nlm.nih.gov/13905658/)
 19. Richardson RB. Age-specific bone tumour incidence rates are governed by stem cell exhaustion influencing the supply and demand of progenitor cells. *Mech Ageing Dev*. 2014; 139:31–40. <https://doi.org/10.1016/j.mad.2014.06.001> PMID:[24927913](https://pubmed.ncbi.nlm.nih.gov/24927913/)
 20. Horvath S. DNA methylation age of human tissues and cell types. *Genome Biol*. 2013; 14:R115. <https://doi.org/10.1186/gb-2013-14-10-r115> PMID:[24138928](https://pubmed.ncbi.nlm.nih.gov/24138928/)
 21. Ogawa T, Kitagawa M, Hirokawa K. Age-related changes of human bone marrow: a histometric estimation of proliferative cells, apoptotic cells, T cells, B cells and macrophages. *Mech Ageing Dev*. 2000; 117:57–68. [https://doi.org/10.1016/s0047-6374\(00\)00137-8](https://doi.org/10.1016/s0047-6374(00)00137-8) PMID:[10958923](https://pubmed.ncbi.nlm.nih.gov/10958923/)
 22. Imaida K, Hasegawa R, Kato T, Futakuchi M, Takahashi S, Ogawa K, Asamoto M, Yamamoto T, Suzuki K, Inagaki T, Shinagawa N, Shirai T. Clinicopathological analysis on cancers of autopsy cases in a geriatric hospital. *Pathol Int*. 1997; 47:293–300. <https://doi.org/10.1111/j.1440-1827.1997.tb04496.x> PMID:[9143024](https://pubmed.ncbi.nlm.nih.gov/9143024/)
 23. Lemaître JF, Pavard S, Giraudeau M, Vincze O, Jennings G, Hamede R, Ujvari B, Thomas F. Eco-evolutionary perspectives of the dynamic relationships linking senescence and cancer. *Functional Ecology*. 2019; 34:1–12. <https://doi.org/10.1111/1365-2435.13394>
 24. Richardson RB, Allan DS, Le Y. Greater organ involution in highly proliferative tissues associated with the early onset and acceleration of ageing in humans. *Exp Gerontol*. 2014; 55:80–91. <https://doi.org/10.1016/j.exger.2014.03.015> PMID:[24685641](https://pubmed.ncbi.nlm.nih.gov/24685641/)
 25. Blagosklonny MV. Aging: ROS or TOR. *Cell Cycle*. 2008; 7:3344–54. <https://doi.org/10.4161/cc.7.21.6965> PMID:[18971624](https://pubmed.ncbi.nlm.nih.gov/18971624/)
 26. Podolskiy DI, Lobanov AV, Kryukov GV, Gladyshev VN. Analysis of cancer genomes reveals basic features of human aging and its role in cancer development. *Nat Commun*. 2016; 7:12157. <https://doi.org/10.1038/ncomms12157> PMID:[27515585](https://pubmed.ncbi.nlm.nih.gov/27515585/)
 27. Feng Z, Levine AJ. The regulation of energy metabolism and the IGF-1/mTOR pathways by the p53 protein. *Trends Cell Biol*. 2010; 20:427–34. <https://doi.org/10.1016/j.tcb.2010.03.004> PMID:[20399660](https://pubmed.ncbi.nlm.nih.gov/20399660/)
 28. Chan JM, Stampfer MJ, Giovannucci E, Gann PH, Ma J, Wilkinson P, Hennekens CH, Pollak M. Plasma insulin-like growth factor-I and prostate cancer risk: a prospective study. *Science*. 1998; 279:563–66. <https://doi.org/10.1126/science.279.5350.563> PMID:[9438850](https://pubmed.ncbi.nlm.nih.gov/9438850/)
 29. Vineis P, Schatzkin A, Potter JD. Models of carcinogenesis: an overview. *Carcinogenesis*. 2010; 31:1703–09. <https://doi.org/10.1093/carcin/bgq087> PMID:[20430846](https://pubmed.ncbi.nlm.nih.gov/20430846/)
 30. Pollak M. Insulin and insulin-like growth factor signalling in neoplasia. *Nat Rev Cancer*. 2008; 8:915–28.

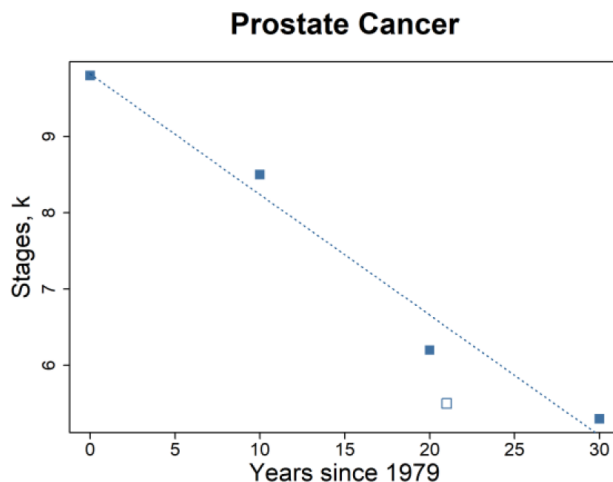
- <https://doi.org/10.1038/nrc2536>
PMID:19029956
31. Vitale G, Pellegrino G, Vollery M, Hofland LJ. Role of IGF-1 system in the modulation of longevity: controversies and new insights from a centenarians' perspective. *Front Endocrinol (Lausanne)*. 2019; 10:27.
<https://doi.org/10.3389/fendo.2019.00027>
PMID:30774624
32. Laron Z, Kauli R, Lapkina L, Werner H. IGF-I deficiency, longevity and cancer protection of patients with Laron syndrome. *Mutat Res Rev Mutat Res*. 2017; 772:123–33.
<https://doi.org/10.1016/j.mrrev.2016.08.002>
PMID:28528685
33. Green J, Cairns BJ, Casabonne D, Wright FL, Reeves G, Beral V, and Million Women Study collaborators. Height and cancer incidence in the Million Women Study: prospective cohort, and meta-analysis of prospective studies of height and total cancer risk. *Lancet Oncol*. 2011; 12:785–94.
[https://doi.org/10.1016/S1470-2045\(11\)70154-1](https://doi.org/10.1016/S1470-2045(11)70154-1)
PMID:21782509
34. Juul A, Bang P, Hertel NT, Main K, Dalgaard P, Jørgensen K, Müller J, Hall K, Skakkebaek NE. Serum insulin-like growth factor-I in 1030 healthy children, adolescents, and adults: relation to age, sex, stage of puberty, testicular size, and body mass index. *J Clin Endocrinol Metab*. 1994; 78:744–52.
<https://doi.org/10.1210/jcem.78.3.8126152>
PMID:8126152
35. Tiryakioğlu O, Kadiolgu P, Canerolgu NU, Hatemi H. Age dependency of serum insulin - like growth factor (IGF)-1 in healthy Turkish adolescents and adults. *Indian J Med Sci*. 2003; 57:543–48.
PMID:14701946
36. Brabant G, von zur Mühlen A, Wüster C, Ranke MB, Kratzsch J, Kiess W, Ketelslegers JM, Wilhelmsen L, Hulthén L, Saller B, Mattsson A, Wilde J, Schemer R, Kann P, and German KIMS Board. Serum insulin-like growth factor I reference values for an automated chemiluminescence immunoassay system: results from a multicenter study. *Horm Res*. 2003; 60:53–60.
<https://doi.org/10.1159/000071871>
PMID:12876414
37. Pontzer H, Yamada Y, Sagayama H, Ainslie PN, Andersen LF, Anderson LJ, Arab L, Baddou I, Bedu-Addo K, Blaak EE, Blanc S, Bonomi AG, Bouten CV, et al, and IAEA DLW Database Consortium. Daily energy expenditure through the human life course. *Science*. 2021; 373:808–12.
<https://doi.org/10.1126/science.abe5017>
PMID:34385400
38. Williams GC. Pleiotrophy, natural selection, and the evolution of senescence. *Evolution*. 1957; 11:398–11.
<https://doi.org/10.2307/2406060>
39. Wright WE, Shay JW. The two-stage mechanism controlling cellular senescence and immortalization. *Exp Gerontol*. 1992; 27:383–89.
[https://doi.org/10.1016/0531-5565\(92\)90069-c](https://doi.org/10.1016/0531-5565(92)90069-c)
PMID:1333985
40. Campisi J, Kim SH, Lim CS, Rubio M. Cellular senescence, cancer and aging: the telomere connection. *Exp Gerontol*. 2001; 36:1619–37.
[https://doi.org/10.1016/s0531-5565\(01\)00160-7](https://doi.org/10.1016/s0531-5565(01)00160-7)
PMID:11672984
41. Sebastiani P, Perls TT. The genetics of extreme longevity: lessons from the New England Centenarian Study. *Front Genet*. 2012; 3:277.
<https://doi.org/10.3389/fgene.2012.00277>
PMID:23226160
42. Herskind AM, McGue M, Holm NV, Sørensen TI, Harvald B, Vaupel JW. The heritability of human longevity: a population-based study of 2872 Danish twin pairs born 1870-1900. *Hum Genet*. 1996; 97:319–23.
<https://doi.org/10.1007/BF02185763> PMID:8786073
43. Berenblum I, Shubik P. An experimental study of the initiating state of carcinogenesis, and a re-examination of the somatic cell mutation theory of cancer. *Br J Cancer*. 1949; 3:109–18.
<https://doi.org/10.1038/bjc.1949.13> PMID:18128325
44. Baylin SB, Jones PA. Epigenetic determinants of cancer. *Cold Spring Harb Perspect Biol*. 2016; 8:a019505.
<https://doi.org/10.1101/cshperspect.a019505>
PMID:27194046
45. Mathon NF, Lloyd AC. Cell senescence and cancer. *Nat Rev Cancer*. 2001; 1:203–13.
<https://doi.org/10.1038/35106045>
PMID:11902575
46. Jiang H, Ju Z, Rudolph KL. Telomere shortening and ageing. *Z Gerontol Geriatr*. 2007; 40:314–24.
<https://doi.org/10.1007/s00391-007-0480-0>
PMID:17943234
47. Brault ME, Autexier C. Telomeric recombination induced by dysfunctional telomeres. *Mol Biol Cell*. 2011; 22:179–88.
<https://doi.org/10.1091/mbc.E10-02-0173>
PMID:21118998
48. Dillekås H, Rogers MS, Straume O. Are 90% of deaths from cancer caused by metastases? *Cancer Med*. 2019; 8:5574–76.
<https://doi.org/10.1002/cam4.2474> PMID:31397113

49. Liao TT, Yang MH. Revisiting epithelial-mesenchymal transition in cancer metastasis: the connection between epithelial plasticity and stemness. *Mol Oncol*. 2017; 11:792–804.
<https://doi.org/10.1002/1878-0261.12096>
PMID:28649800
50. Joyce JA, Pollard JW. Microenvironmental regulation of metastasis. *Nat Rev Cancer*. 2009; 9:239–52.
<https://doi.org/10.1038/nrc2618>
PMID:19279573
51. Keymer JE, Marquet PA. The complexity of cancer ecosystems. In: Benitez M, Miramontes O and Valiente-Banuet A, eds. *Frontiers in Ecology, Evolution and Complexity*. (Mexico City: Coplt-arXives). 2014.
<https://doi.org/10.13140/2.1.3757.2805>
52. Mayer S, Brüderlein S, Perner S, Waibel I, Holdenried A, Ciloglu N, Hasel C, Mattfeldt T, Nielsen KV, Möller P. Sex-specific telomere length profiles and age-dependent erosion dynamics of individual chromosome arms in humans. *Cytogenet Genome Res*. 2006; 112:194–201.
<https://doi.org/10.1159/000089870> PMID:16484772
53. Palmer S, Albergante L, Blackburn CC, Newman TJ. Thymic involution and rising disease incidence with age. *Proc Natl Acad Sci USA*. 2018; 115:1883–88.
<https://doi.org/10.1073/pnas.1714478115>
PMID:29432166
54. Hwang SJ, Lozano G, Amos CI, Strong LC. Germline p53 mutations in a cohort with childhood sarcoma: sex differences in cancer risk. *Am J Hum Genet*. 2003; 72:975–83.
<https://doi.org/10.1086/374567> PMID:12610779
55. Nunney L, Thai K. Determining cancer risk: the evolutionary multistage model or total stem cell divisions? *Proc Biol Sci*. 2020; 287:20202291.
<https://doi.org/10.1098/rspb.2020.2291>
PMID:33323077
56. Gerstung M, Jolly C, Leshchiner I, Dentre SC, Gonzalez S, Rosebrock D, Mitchell TJ, Rubanova Y, Anur P, Yu K, Tarabichi M, Deshwar A, Wintersinger J, et al, and PCAWG Evolution and Heterogeneity Working Group, and PCAWG Consortium. The evolutionary history of 2,658 cancers. *Nature*. 2020; 578:122–28.
<https://doi.org/10.1038/s41586-019-1907-7>
PMID:32025013
57. Fidler IJ. Metastasis: quantitative analysis of distribution and fate of tumor emboli labeled with 125 I-5-iodo-2'-deoxyuridine. *J Natl Cancer Inst*. 1970; 45:773–82.
PMID:5513503
58. Reiter JG, Makohon-Moore AP, Gerold JM, Heyde A, Attiyeh MA, Kohutek ZA, Tokheim CJ, Brown A, DeBlasio RM, Niyazov J, Zucker A, Karchin R, Kinzler KW, et al. Minimal functional driver gene heterogeneity among untreated metastases. *Science*. 2018; 361:1033–37.
<https://doi.org/10.1126/science.aat7171>
PMID:30190408
59. Metzeler KH, Herold T, Rothenberg-Thurley M, Amler S, Sauerland MC, Görlich D, Schneider S, Konstandin NP, Dufour A, Bräundl K, Ksienzyk B, Zellmeier E, Hartmann L, et al, and AMLCG Study Group. Spectrum and prognostic relevance of driver gene mutations in acute myeloid leukemia. *Blood*. 2016; 128:686–98.
<https://doi.org/10.1182/blood-2016-01-693879>
PMID:27288520
60. Richardson RB. p53 mutations associated with aging-related rise in cancer incidence rates. *Cell Cycle*. 2013; 12:2468–78.
<https://doi.org/10.4161/cc.25494> PMID:23839036
61. Nik-Zainal S, Van Loo P, Wedge DC, Alexandrov LB, Greenman CD, Lau KW, Raine K, Jones D, Marshall J, Ramakrishna M, Shlien A, Cooke SL, Hinton J, et al, and Breast Cancer Working Group of the International Cancer Genome Consortium. The life history of 21 breast cancers. *Cell*. 2012; 149:994–1007.
<https://doi.org/10.1016/j.cell.2012.04.023>
PMID:22608083
62. Zhao ZM, Zhao B, Bai Y, Iamarino A, Gaffney SG, Schlessinger J, Lifton RP, Rimm DL, Townsend JP. Early and multiple origins of metastatic lineages within primary tumors. *Proc Natl Acad Sci USA*. 2016; 113:2140–45.
<https://doi.org/10.1073/pnas.1525677113>
PMID:26858460
63. Bizzarri M, Cucina A, Conti F, D'Anselmi F. Beyond the oncogene paradigm: understanding complexity in cancerogenesis. *Acta Biotheor*. 2008; 56:173–96.
<https://doi.org/10.1007/s10441-008-9047-8>
PMID:18288572
64. Moolgavkar SH, Venzon DJ. Two-event models for carcinogenesis: incidence curves for childhood and adult tumors. *Mathematical Biosciences*. 1979; 47:55–77.
[https://doi.org/10.1016/0025-5564\(79\)90005-1](https://doi.org/10.1016/0025-5564(79)90005-1)
65. Knudson AG Jr. Mutation and cancer: statistical study of retinoblastoma. *Proc Natl Acad Sci USA*. 1971; 68:820–23.
<https://doi.org/10.1073/pnas.68.4.820>
PMID:5279523
66. Richardson RB. Promotional etiology for common childhood acute lymphoblastic leukemia: the infective lymphoid recovery hypothesis. *Leuk Res*. 2011; 35:1425–31.

- <https://doi.org/10.1016/j.leukres.2011.07.023>
PMID:[21903265](https://pubmed.ncbi.nlm.nih.gov/21903265/)
67. Choo Z, Loh AH, Chen ZX. Destined to die: apoptosis and pediatric cancers. *Cancers (Basel)*. 2019; 11:1623.
<https://doi.org/10.3390/cancers11111623>
PMID:[31652776](https://pubmed.ncbi.nlm.nih.gov/31652776/)
68. Little MP. Cancer models, genomic instability and somatic cellular Darwinian evolution. *Biol Direct*. 2010; 5:19; discussion 19.
<https://doi.org/10.1186/1745-6150-5-19>
PMID:[20406436](https://pubmed.ncbi.nlm.nih.gov/20406436/)
69. Cook PJ, Doll R, Fellingham SA. A mathematical model for the age distribution of cancer in man. *Int J Cancer*. 1969; 4:93–112.
<https://doi.org/10.1002/ijc.2910040113>
PMID:[5346480](https://pubmed.ncbi.nlm.nih.gov/5346480/)
70. Ritter G, Wilson R, Pompei F, Burmistrov D. The multistage model of cancer development: some implications. *Toxicol Ind Health*. 2003; 19:125–45.
<https://doi.org/10.1191/0748233703th195oa>
PMID:[15747774](https://pubmed.ncbi.nlm.nih.gov/15747774/)
71. Belikov AV. The number of key carcinogenic events can be predicted from cancer incidence. *Sci Rep*. 2017; 7:12170.
<https://doi.org/10.1038/s41598-017-12448-7>
PMID:[28939880](https://pubmed.ncbi.nlm.nih.gov/28939880/)
72. Vogelstein B, Kinzler KW. The path to cancer --three strikes and you're out. *N Engl J Med*. 2015; 373:1895–98.
<https://doi.org/10.1056/NEJMp1508811>
PMID:[26559569](https://pubmed.ncbi.nlm.nih.gov/26559569/)
73. Etzioni R, Penson DF, Legler JM, di Tommaso D, Boer R, Gann PH, Feuer EJ. Overdiagnosis due to prostate-specific antigen screening: lessons from U.S. prostate cancer incidence trends. *J Natl Cancer Inst*. 2002; 94:981–90.
<https://doi.org/10.1093/jnci/94.13.981>
PMID:[12096083](https://pubmed.ncbi.nlm.nih.gov/12096083/)
74. Glasziou PP, Jones MA, Pathirana T, Barratt AL, Bell KJ. Estimating the magnitude of cancer overdiagnosis in Australia. *Med J Aust*. 2020; 212:163–68.
<https://doi.org/10.5694/mja2.50455>
PMID:[31858624](https://pubmed.ncbi.nlm.nih.gov/31858624/)
75. Hanson HA, Smith KR, Stroup AM, Harrell CJ. An age-period-cohort analysis of cancer incidence among the oldest old, Utah 1973–2002. *Popul Stud (Camb)*. 2015; 69:7–22.
<https://doi.org/10.1080/00324728.2014.958192>
PMID:[25396304](https://pubmed.ncbi.nlm.nih.gov/25396304/)
76. Wang X, Steensma JT, Bailey MH, Feng Q, Padda H, Johnson KJ. Characteristics of The Cancer Genome Atlas cases relative to U.S. general population cancer cases. *Br J Cancer*. 2018; 119:885–92.
<https://doi.org/10.1038/s41416-018-0140-8>
PMID:[30131556](https://pubmed.ncbi.nlm.nih.gov/30131556/)
77. Miller B, Feuer E, Altekruse S. Cancer incidence patterns in the oldest ages using expanded age categories from SEER Registry Data and the 2010 Census Population. *J Registry Manag*. 2017; 44:130–35.
PMID:[30133428](https://pubmed.ncbi.nlm.nih.gov/30133428/)
78. R Core Team. A language and environment for statistical computing (Vienna, Austria: R Foundation for Statistical Computing). 2020. <https://www.R-project.org/>.
79. Elzhov TV, Mullen KM, Spiess AN, Bolker B. Package 'minpack.lm'. In: R interface to the Levenberg-Marquardt nonlinear least-squares algorithm found in MINPACK psfb, ed.: CRAN). 2016. <https://CRAN.R-project.org/package=minpack.lm>
80. Pompei F, Wilson R. A quantitative model of cellular senescence influence on cancer and longevity. *Toxicol Ind Health*. 2002; 18:365–76.
<https://doi.org/10.1191/0748233702th164oa>
PMID:[15119525](https://pubmed.ncbi.nlm.nih.gov/15119525/)
81. Martincorena I, Raine KM, Gerstung M, Dawson KJ, Haase K, Van Loo P, Davies H, Stratton MR, Campbell PJ. Universal patterns of selection in cancer and somatic tissues. *Cell*. 2017; 171:1029–41.e21.
<https://doi.org/10.1016/j.cell.2017.09.042>
PMID:[29056346](https://pubmed.ncbi.nlm.nih.gov/29056346/)

SUPPLEMENTARY MATERIALS

Supplementary Figure



Supplementary Figure 1. Stage k for prostate cancer versus timeline for SEER data from the 1979–1983, 1989–1993, and 1999–2003 studies (Harding, Pompei et al. 2008) and the corresponding data for 2010–2013 from Supplementary Table 4A. Data for 2000–2003 is shown as an outlined square (Supplementary Table 5A), for comparison with 1999–2003 data, but is not included in the regression line fits due to the overlap in data sets.

Supplementary Tables

Supplementary Table 1A. Male (M) parameter values of model-fits to SEER 2010–2013 age-specific cancer incidence rates for reproductive and non-reproductive cancer types, employing the multistage-senescence model (Equation 5).

Sex	Cancer type (TCGA) ⁰	Model-fitted ¹			P values			Peak incidence rate (per 100,000 person-year)		Age of peak incidence (yr)		Cumulative probability over lifespan			Ratio of cum. prob., SEER/2-variable
		u_{μ} (yr ⁻¹)	k	b (yr ⁻¹)	u	k	b	SEER	Model-fitted ²	SEE R	Model-fitted ³	SEER	Model-fitted ⁴	2-Variable model fitted	
M	ACC	0.011	6.44	0.0107	3.60E-05	1.30E-07	5.50E-14	0.347	0.301	87.5	79.2	0.00012	9.50E-05	0.01	0.011
M	BLCA	0.04	9	0.0098	7.50E-12	3.60E-12	2.50E-15	344	380	92.5	91	0.1	0.1	0.017	6.1
M	COAD	0.029	6.9	0.0094	1.40E-10	3.00E-11	3.30E-13	228	230	92.5	90.9	0.08	0.078	0.023	3.5
M	COADREAD	0.027	6.19	0.0092	8.60E-10	2.10E-10	6.20E-12	274	279	92.5	91.2	0.1	0.11	0.026	3.9
M	ESCA	0.025	6.91	0.0101	5.00E-08	5.10E-09	2.90E-13	42.5	47.4	82.5	84.9	0.016	0.015	0.014	1.1
M	GBM	0.019	6.16	0.0103	2.00E-09	1.10E-10	2.70E-16	19.7	19.3	77.5	81.7	0.0067	0.0065	0.013	0.5
M	HNSC	0.019	5.07	0.01	1.00E-07	2.30E-08	1.00E-12	110	90.4	102.5	80.6	0.041	0.037	0.017	2.4
M	KICH	0.014	5.88	0.0106	1.90E-06	3.20E-08	4.10E-15	4.13	3.65	72.5	78.2	0.0013	0.0012	0.011	0.12
M	KIRC	0.017	5.13	0.0105	1.40E-06	2.70E-07	4.10E-15	41.9	37.9	72.5	76.9	0.014	0.014	0.013	1
M	KIRP	0.016	5.62	0.0106	2.00E-05	1.20E-06	1.30E-14	13.5	11.4	72.5	77.2	0.0039	0.004	0.011	0.34
M	LAML	0.03	8.37	0.0098	6.70E-12	5.30E-13	2.20E-16	42	45.5	87.5	89.5	0.014	0.013	0.016	0.85
M	LGG	9.20E-05	1.52	0.0085	8.80E-01	7.70E-01	8.40E-02	0.502	0.363	82.5	40.3	0.0003	0.0003	0.032	0.0094
M	LIHC	0.015	4.57	0.0102	3.50E-04	7.60E-05	2.30E-10	47.3	46.1	62.5	76.7	0.018	0.02	0.017	1.1
M	LUAD	0.035	7.81	0.0102	3.90E-09	2.40E-09	7.00E-15	202	206	82.5	85.6	0.059	0.058	0.012	4.8
M	LUSC	0.035	8.4	0.0102	5.40E-08	2.50E-08	1.60E-14	135	134	82.5	85.9	0.036	0.036	0.011	3.1
M	MESO	0.038	11.42	0.01	1.90E-10	1.10E-11	9.70E-16	11	12.7	92.5	91.5	0.0027	0.0027	0.014	0.19
M	PAAD	0.027	7.09	0.0101	1.00E-09	2.30E-10	1.00E-15	74.9	75.7	82.5	85.1	0.023	0.023	0.014	1.7
M	PCPG	7.00E-06	1.33	-0.0168	1.00E+00	1.00E+00	1.00E+00	0.407	NaN	92.5	-14.8	9.30E-05	NaN	NaN	NaN
M	READ	0.014	4.49	0.0089	1.60E-07	6.80E-09	1.60E-10	51	49.9	97.5	87.8	0.023	0.025	0.031	0.73
M	SARC	0.015	6.4	0.0071	4.70E-03	6.20E-05	1.70E-02	12.6	24.4	87.5	119	0.0042	0.012	0.13	0.031
M	SKCM	0.027	6.52	0.0093	3.90E-11	6.20E-12	1.40E-13	220	195	102.5	91	0.075	0.07	0.024	3.1
M	STAD	0.026	7.24	0.0096	3.00E-12	2.10E-13	1.30E-15	71.4	70.2	97.5	90.2	0.024	0.023	0.02	1.2
M	THCA	0.011	4.14	0.0103	1.20E-07	6.80E-09	1.30E-15	19.8	18.3	72.5	73.6	0.0087	0.0082	0.017	0.52
M	THYM	0.012	6.11	0.0107	7.10E-05	5.20E-07	1.00E-13	1	0.795	82.5	78.1	0.00028	0.00026	0.01	0.027
M	PRAD	0.035	5.11	0.0125	2.60E-06	9.90E-06	2.40E-11	746	642	72.5	79.5	0.22	0.21	0.0055	40
M	TGCT	0.0013	1.52	0.0237	8.00E-02	2.90E-02	2.70E-05	14.7	12.5	27.5	29.3	0.004	0.0036	0.0067	0.6

⁰Non-reproductive cancers: ACC adrenocortical carcinoma, BLCA bladder urothelial carcinoma, COAD colon adenocarcinoma, COADREAD both COAD and READ cases, ESCA esophageal carcinoma, GBM glioblastoma multiforme, HNSC head and neck squamous cell carcinoma, KICH kidney chromophobe, KIRC kidney renal clear cell carcinoma, KIRP kidney renal papillary cell carcinoma, LAML acute myeloid leukemia, LGG brain lower grade glioma, LIHC liver hepatocellular carcinoma, LUAD lung adenocarcinoma, LUSC lung squamous cell carcinoma, MESO mesothelioma, PAAD pancreatic adenocarcinoma, PCPG pheochromocytoma and paraganglioma, READ rectum adenocarcinoma, SARC sarcoma, SKCM skin cutaneous melanoma, STAD stomach adenocarcinoma, THYM thymoma, THCA thyroid carcinoma.

Male reproductive cancers: PRAD prostate adenocarcinoma, TGCT testicular germ cell tumors.

Other abbreviations: NaN Not a Number.

¹Equation 5; ²Equation 6; ³Equation 6 substituted in Equation 5; ⁴Equation 7.

The peak age-specific incidence rate, age of peak incidence rate, and cumulative probability of cancer over life span are computed up to maximum age 105, based on the SEER data alternatively model-fitted $ASR(t)$. The age-specific incidence rate is computed per 100,000 population for each five-year age group. LGG and PCPG are cancer types with P values for model-fitted u_{μ} or k larger than 0.1 and were omitted from further analysis.

Supplementary Table 1B. Female (F) parameter values of model-fits to SEER 2010–2013 age-specific cancer incidence rates for reproductive and non-reproductive cancer types, employing the multistage-senescence model (Equation 5).

Sex	Cancer type (TCGA) ⁰	Model-fitted ¹			P values			Peak incidence rate (per 100,000 person-year)		Age of peak incidence (yr)		Cumulative probability over lifespan			Ratio of cum. prob., SEER/2-variable
		u_{μ} (yr ⁻¹)	k	b (yr ⁻¹)	u	k	b	SEER	Model-fitted ²	SEER	Model-fitted ³	SEER	Model-fitted ⁴	2-Variable model fitted	
F	ACC	0.005	4.42	0.0105	1.60E-03	6.00E-06	3.70E-13	0.396	0.343	77.5	73.7	0.00015	0.00014	0.0077	0.02
F	BLCA	0.03	8.08	0.0097	1.10E-10	1.50E-11	1.70E-15	64.6	72.7	92.5	90.2	0.022	0.021	0.0071	3.1
F	COAD	0.03	7.23	0.0095	2.90E-09	9.40E-10	2.50E-13	193	188	87.5	90.2	0.062	0.061	0.0086	7.2
F	COADREAD	0.028	6.55	0.0093	6.50E-08	2.00E-08	2.70E-11	220	213	87.5	90.6	0.075	0.076	0.01	7.1
F	ESCA	0.02	7.09	0.0098	6.10E-10	1.70E-11	1.60E-15	11.7	12.1	87.5	88.1	0.0043	0.0039	0.0075	0.58
F	GBM	0.015	5.56	0.0101	5.20E-07	2.00E-08	9.50E-15	12.6	11.1	77.5	81.4	0.0042	0.0042	0.0075	0.56
F	HNSC	0.015	5.13	0.0092	9.70E-10	3.20E-11	4.70E-14	31.4	29.5	92.5	87.1	0.013	0.013	0.013	1
F	KICH	0.0083	4.74	0.0104	6.20E-04	8.00E-06	4.20E-13	2.21	1.86	77.5	75.6	0.00081	0.00075	0.0074	0.11
F	KIRC	0.013	4.63	0.0104	7.30E-05	9.00E-06	1.70E-15	23.2	18	72.5	75.6	0.0073	0.0075	0.0078	0.94
F	KIRP	0.011	5.22	0.0105	1.50E-04	3.00E-06	3.90E-14	3.56	2.98	77.5	77.3	0.0011	0.0011	0.0065	0.17
F	LAML	0.023	7.33	0.0097	2.90E-09	1.40E-10	1.50E-14	22	23.1	82.5	88.8	0.0082	0.0072	0.0075	1.1
F	LGG	0.00093	2.65	0.0101	5.60E-01	1.90E-01	6.90E-06	0.364	0.213	32.5	61.4	0.00022	0.00013	0.013	0.017
F	LIHC	0.018	6.06	0.0101	6.00E-08	3.50E-09	1.10E-15	17.3	16.2	82.5	82.4	0.0057	0.0056	0.0067	0.85
F	LUAD	0.029	6.73	0.0101	1.90E-07	1.30E-07	1.70E-14	162	144	77.5	84	0.047	0.046	0.006	7.8
F	LUSC	0.028	7.65	0.0102	6.80E-06	2.10E-06	8.60E-15	69	51.9	77.5	85.3	0.016	0.015	0.0051	3.1
F	MESO	0.018	7.85	0.0091	4.00E-05	2.80E-07	2.40E-08	2.29	2.15	102.5	96.3	0.00065	0.00068	0.012	0.052
F	PAAD	0.027	7.18	0.01	7.80E-09	1.70E-09	1.60E-15	60.7	59.5	82.5	86	0.019	0.018	0.0062	3
F	PCPG	0.004	4.45	0.0109	2.20E-01	1.60E-02	5.80E-09	0.182	0.111	72.5	71.1	6.10E-05	4.50E-05	0.0064	0.0094
F	READ	0.0043	2.82	0.0038	4.10E-01	1.50E-01	6.80E-01	28.3	49.3	82.5	170	0.013	0.076	0.2	0.063
F	SARC	0.0093	5.01	0.0077	5.60E-05	2.00E-07	1.80E-06	7.67	6.65	97.5	104	0.0023	0.0035	0.031	0.074
F	SKCM	0.012	4.08	0.0083	4.20E-06	2.20E-07	1.30E-08	59.4	58.8	82.5	91	0.029	0.033	0.022	1.3
F	STAD	0.022	6.98	0.0094	2.00E-08	9.10E-10	2.10E-12	34.4	33.1	102.5	91.2	0.012	0.011	0.0099	1.2
F	THCA	0.0053	2.36	0.0102	9.20E-09	7.10E-10	5.10E-19	38.3	36.6	52.5	56.3	0.022	0.022	0.013	1.7
F	THYM	0.0087	5.34	0.0107	1.20E-04	8.20E-07	8.20E-17	0.793	0.658	67.5	75.7	0.00025	0.00024	0.0056	0.045
F	BRCA	0.023	3.72	0.0115	1.20E-09	4.60E-09	9.00E-14	435	428	77.5	78.5	0.19	0.18	0.0065	30
F	CESC	0.0011	1.57	0.0105	1.50E-03	9.00E-05	2.50E-10	13.8	11.9	42.5	49.5	0.0071	0.0078	0.0094	0.76
F	OV	0.011	4.07	0.0121	1.20E-06	2.60E-08	8.30E-15	12.7	11.9	72.5	77.5	0.0045	0.0046	0.0048	0.96
F	UCEC	0.013	3.4	0.0121	8.60E-05	3.00E-05	1.00E-11	84	73.1	67.5	73.2	0.03	0.032	0.0061	5
F	UCS	0.01	5.59	0.0125	3.70E-03	3.00E-05	6.60E-11	0.711	0.519	82.5	80.6	0.00018	0.00016	0.0022	0.081

⁰Female reproductive cancers: BRCA breast invasive carcinoma, CESC cervical squamous cell carcinoma and endocervical adenocarcinoma, OV ovarian serous cystadenocarcinoma, UCEC uterine corpus endometrial carcinoma, UCS uterine carcinosarcoma.

Abbreviations for non-reproductive cancer types and footnotes 1-4 are explained in Supplementary Table 1A. LGG, PCPG and READ are cancer types with P values for model-fitted u_{μ} or k larger than 0.1 and were omitted from further analysis.

Supplementary Table 1C. Both sexes pooled (M&F) parameter values of model-fits to SEER 2010–2013 age-specific cancer incidence rates for non-reproductive cancer types only, employing the multistage-senescence model (Equation 5).

Sex	Cancer type (TCGA) ⁰	Model-fitted ¹			P values			Peak incidence rate (per 100,000 person-year)		Age of peak incidence (yr)		Cumulative probability over lifespan			Ratio of cum. prob., SEER/2-variable
		u_{μ} (yr ⁻¹)	k	b (yr ⁻¹)	u	k	b	SEER	Model-fitted ²	SEER	Model-fitted ³	SEER	Model-fitted ⁴	2-Variable model fitted	
		M&F	ACC	0.0067	5.1	0.0105	9.30E-06	1.80E-08	1.70E-15	0.329	0.319	77.5	76.6	0.00014	
M&F	BLCA	0.036	8.47	0.0098	1.30E-10	5.20E-11	1.80E-15	161	183	87.5	89.6	0.052	0.05	0.013	4.1
M&F	COAD	0.03	7.03	0.0095	4.20E-10	1.20E-10	1.00E-13	203	203	87.5	90.1	0.068	0.067	0.014	5
M&F	COADREAD	0.027	6.32	0.0093	4.80E-09	1.50E-09	4.30E-12	238	235	87.5	90.2	0.084	0.086	0.014	6
M&F	ESCA	0.022	6.64	0.01	4.50E-08	3.10E-09	3.50E-14	24.1	26	82.5	84.7	0.009	0.0085	0.0092	0.98
M&F	GBM	0.016	5.65	0.0101	1.50E-07	7.20E-09	4.30E-15	15.7	14.3	77.5	81.6	0.0052	0.0053	0.0082	0.63
M&F	HNSC	0.017	4.87	0.0098	9.20E-08	1.20E-08	2.80E-13	52.6	54.3	77.5	80.9	0.024	0.023	0.0088	2.7
M&F	KICH	0.01	5.17	0.0105	4.50E-05	6.10E-07	1.90E-14	3.05	2.58	72.5	77	0.001	0.00098	0.0065	0.16
M&F	KIRC	0.014	4.69	0.0104	2.40E-05	4.10E-06	2.90E-15	31.7	26.1	72.5	75.8	0.01	0.011	0.0066	1.5
M&F	KIRP	0.012	5.05	0.0105	2.40E-04	1.00E-05	6.00E-14	8.04	6.33	72.5	76.4	0.0024	0.0024	0.0064	0.37
M&F	LAML	0.026	7.77	0.0098	2.40E-10	1.70E-11	1.30E-15	29.6	31.4	82.5	88.8	0.01	0.0093	0.012	0.85
M&F	LGG	0.00064	2.34	0.0099	5.00E-01	1.40E-01	2.10E-06	0.404	0.279	32.5	57.9	0.00026	0.00018	0.0026	0.1
M&F	LIHC	0.014	4.69	0.0102	6.00E-05	7.80E-06	3.00E-12	28.4	28.7	77.5	77.5	0.011	0.012	0.0073	1.5
M&F	LUAD	0.03	7.07	0.0101	7.10E-08	4.80E-08	2.10E-14	177	165	77.5	85	0.051	0.051	0.0091	5.7
M&F	LUSC	0.03	7.69	0.0101	1.60E-06	6.20E-07	3.30E-14	95.8	81.4	77.5	85.8	0.024	0.023	0.0092	2.6
M&F	MESO	0.03	10.2	0.0099	8.60E-10	3.10E-11	4.50E-16	5.09	5.69	87.5	90.8	0.0014	0.0013	0.014	0.1
M&F	PAAD	0.026	7.02	0.01	5.40E-09	1.20E-09	2.00E-15	66.5	65.7	82.5	85.5	0.02	0.021	0.0095	2.2
M&F	PCPG	0.0032	4.11	0.0103	1.00E-01	2.00E-03	1.80E-08	0.188	0.133	92.5	73.4	7.30E-05	6.00E-05	0.0065	0.011
M&F	READ	0.011	4.12	0.0087	1.50E-05	5.80E-07	8.10E-09	37	35.8	82.5	87.5	0.016	0.019	0.013	1.2
M&F	SARC	0.014	6.06	0.0084	2.10E-06	1.30E-08	1.80E-08	8.74	8.96	97.5	98.9	0.0029	0.0037	0.025	0.12
M&F	SKCM	0.021	5.67	0.0094	1.50E-10	2.20E-11	3.00E-14	107	107	82.5	87.9	0.045	0.043	0.013	3.6
M&F	STAD	0.024	7.02	0.0096	5.40E-11	3.50E-12	3.00E-15	43.3	46.5	87.5	89.5	0.016	0.015	0.013	1.3
M&F	THCA	0.0059	2.69	0.0101	1.10E-04	2.10E-05	2.40E-13	28.6	26.4	67.5	62.4	0.016	0.016	0.0042	3.7
M&F	THYM	0.0094	5.54	0.0106	4.20E-05	2.60E-07	6.80E-16	0.747	0.705	67.5	77	0.00026	0.00025	0.0061	0.043
M	Mean	0.0231	6.8	0.0100				42.3	45.8	82.5	85.0	0.015	0.015	0.014	1.06
M	SD	0.0092	1.7	0.0008				95.9	99.6	10.7	9.8	0.030	0.029	0.027	1.73
F	Mean	0.0174	5.9	0.0098				22.6	20.6	82.5	85.6	0.0078	0.0073	0.0075	0.97
F	SD	0.0084	1.5	0.0008				52.1	49.4	11.8	10.0	0.016	0.016	0.062	2.22
μ_M, μ_F^5	<i>t test, P</i>	0.000056	0.0033	0.034 [*]				0.014 [†]	0.012 [†]	0.45	0.32	0.012 [†]	0.0094 [†]	0.035 [*]	0.73

⁵The mean, SD and paired *t*-test *P* values in each column are for the 20 non-reproductive, paired cancer types for males and females, for the parameter in the corresponding column.

[†]Values are no longer significant to 5% level when Holm's method for multiple-testing correction is applied for the paired *t* tests in the table

^{*}Values are no longer significant to 10% level when Holm's method for multiple-testing correction is applied for the paired *t* tests in the table.

Male (M) and female (F) parameter values are compared by paired *t* test for 20 paired cancer types in the last row of the table.

Abbreviations for non-reproductive cancer types (footnote 0) and footnotes 1-4 are explained in Supplementary Table 1A. LGG and PCPG are cancer types with *P* values for model-fitted u_{μ} or k larger than 0.1 and were omitted from further analysis.

Supplementary Table 2A. Male (M) parameter values of model-fits to SEER 2000–2003 age-specific cancer incidence rates for reproductive and non-reproductive cancer types, employing the multistage-senescence model (Equation 5).

Sex	Cancer type (TCGA) ⁰	Model-fitted ¹			<i>P</i> values			Peak incidence rate (per 100,000 person-year)		Age of peak incidence (yr)		Cumulative probability over lifespan			Ratio of cum. prob., SEER/2-variable
		u_{μ} (yr ⁻¹)	<i>k</i>	<i>b</i> (yr ⁻¹)	<i>u</i>	<i>k</i>	<i>b</i>	SEER	Model-fitted ²	SEER	Model-fitted ³	SEER	Model-fitted ⁴	2-Variable model fitted	
M	ACC	0.0077	5.43	0.0106	9.20E-02	3.90E-03	3.00E-07	0.456	0.289	72.5	76.6	0.00014	0.0001	0.01	0.014
M	BLCA	0.037	8.2	0.0096	7.80E-11	4.20E-11	5.40E-14	322	363	87.5	91.2	0.1	0.1	0.023	4.3
M	COAD	0.035	7.63	0.0096	7.20E-12	3.70E-12	9.30E-15	346	374	87.5	91	0.11	0.12	0.023	4.8
M	COADREAD	0.034	7.22	0.0096	3.60E-12	2.40E-12	5.60E-15	420	442	87.5	90.1	0.14	0.14	0.022	6.2
M	ESCA	0.024	6.59	0.0101	1.80E-09	1.90E-10	8.60E-15	50.2	48	102.5	84.2	0.018	0.016	0.014	1.3
M	GBM	0.019	6.08	0.0102	2.50E-08	1.30E-09	9.80E-15	18.9	18.7	77.5	81.5	0.0066	0.0064	0.013	0.52
M	HNSC	0.019	5.04	0.0099	1.50E-07	3.30E-08	2.60E-12	86.9	92.2	72.5	80.7	0.039	0.038	0.014	2.7
M	KICH	0.014	6.31	0.0106	1.30E-07	1.10E-09	5.10E-16	1.93	1.72	77.5	79.5	0.00056	0.00056	0.01	0.054
M	KIRC	0.015	5.07	0.0104	3.10E-07	2.80E-08	8.00E-16	21.9	20.3	72.5	77.2	0.0073	0.0078	0.012	0.63
M	KIRP	0.015	5.87	0.0107	4.30E-07	1.10E-08	1.00E-16	5.17	5.02	72.5	77.6	0.0016	0.0017	0.0099	0.16
M	LAML	0.028	8.09	0.0099	5.00E-12	3.90E-13	1.10E-16	38	39.1	87.5	88.6	0.012	0.011	0.018	0.67
M	LGG	0.00026	1.71	0.0073	8.10E-01	6.40E-01	2.10E-01	1.07	0.864	77.5	56.8	0.00072	0.00082	0.0044	0.16
M	LIHC	0.015	4.97	0.01	4.50E-08	3.10E-09	5.40E-14	32.2	30.6	77.5	79.9	0.012	0.012	0.014	0.85
M	LUAD	0.031	7.17	0.0102	6.40E-08	4.00E-08	1.20E-13	168	172	77.5	84.1	0.052	0.052	0.013	3.9
M	LUSC	0.033	7.84	0.0103	5.60E-07	3.00E-07	3.80E-13	139	136	77.5	85	0.038	0.038	0.013	2.8
M	MESO	0.033	10.02	0.0102	3.70E-08	2.50E-09	9.10E-14	12.6	14.8	82.5	88.6	0.004	0.0034	0.017	0.23
M	PAAD	0.026	6.97	0.0102	5.50E-09	1.00E-09	4.00E-15	55.4	57.5	82.5	83.7	0.018	0.018	0.013	1.4
M	PCPG	2.60E-10	0.47	0.0092	9.90E-01	8.90E-01	3.70E-01	0.326	NaN	92.5	-124	7.50E-05	0.00023	NaN	NaN
M	READ	0.023	6.2	0.0098	5.60E-12	7.80E-13	1.60E-16	73.8	75.2	87.5	85.2	0.026	0.026	0.016	1.6
M	SARC	0.017	6.82	0.0088	2.90E-04	3.10E-06	4.50E-06	7.67	7.57	97.5	97.3	0.0022	0.0028	0.038	0.058
M	SKCM	0.02	5.39	0.009	1.60E-11	1.50E-12	8.10E-14	123	123	92.5	90.3	0.05	0.053	0.025	2
M	STAD	0.028	7.51	0.0096	2.20E-11	2.00E-12	2.20E-14	100	90.2	102.5	90.8	0.032	0.028	0.023	1.4
M	THCA	0.009	3.97	0.0103	2.10E-07	5.60E-09	3.10E-15	11.8	11.1	67.5	72.8	0.0053	0.0052	0.012	0.44
M	THYM	0.0093	5.52	0.0104	2.10E-05	7.60E-08	6.10E-13	0.884	0.756	82.5	78.6	0.00029	0.00027	0.011	0.026
M	PRAD	0.038	5.44	0.012	3.00E-07	1.50E-06	1.10E-10	1020	1010	72.5	83.1	0.33	0.32	0.0053	61
M	TGCT	0.0019	1.69	0.0238	1.00E-02	1.90E-03	3.10E-06	12.6	11.6	32.5	32.2	0.0037	0.0034	0.00054	6.8

⁰Non-reproductive cancers: ACC adrenocortical carcinoma, BLCA bladder urothelial carcinoma, COAD colon adenocarcinoma, COADREAD both COAD and READ cases, ESCA esophageal carcinoma, GBM glioblastoma multiforme, HNSC head and neck squamous cell carcinoma, KICH kidney chromophobe, KIRC kidney renal clear cell carcinoma, KIRP kidney renal papillary cell carcinoma, LAML acute myeloid leukemia, LGG brain lower grade glioma, LIHC liver hepatocellular carcinoma, LUAD lung adenocarcinoma, LUSC lung squamous cell carcinoma, MESO mesothelioma, PAAD pancreatic adenocarcinoma, PCPG pheochromocytoma and paraganglioma, READ rectum adenocarcinoma, SARC sarcoma, SKCM skin cutaneous melanoma, STAD stomach adenocarcinoma, THYM thymoma, THCA thyroid carcinoma.

Male reproductive cancers: PRAD prostate adenocarcinoma, TGCT testicular germ cell tumors.

Other abbreviations: NaN Not a Number.

¹Equation 5; ²Equation 6; ³Equation 6 substituted in Equation 5; ⁴Equation 7.

The peak age-specific incidence rate, age of peak incidence rate, and cumulative probability of cancer over life span are computed up to maximum age 105, based on the SEER data alternatively model-fitted $ASR(t)$. The age-specific incidence rate is computed per 100,000 population for each five-year age group. LGG and PCPG are cancer types with *P* values for model-fitted u_{μ} or *k* larger than 0.1 and were omitted from further analysis.

Supplementary Table 2B. Female (F) parameter values of model-fits to SEER 2000–2003 age-specific cancer incidence rates for reproductive and non-reproductive cancer types, employing the multistage-senescence model (Equation 5).

Sex	Cancer type (TCGA) ⁰	Model-fitted ¹			<i>P</i> values			Peak incidence rate (per 100,000 person-year)		Age of peak incidence (yr)		Cumulative probability over lifespan			Ratio of cum. prob., SEER/2-variable
		u_{μ} (yr ⁻¹)	<i>k</i>	<i>b</i> (yr ⁻¹)	<i>u</i>	<i>k</i>	<i>b</i>	SEER	Model-fitted ²	SEER	Model-fitted ³	SEER	Model-fitted ⁴	2-Variable model fitted	
F	ACC	0.0019	3.2	0.0105	2.30E-01	1.70E-02	8.40E-09	0.383	0.24	62.5	65.4	0.00013	0.00012	0.011	0.011
F	BLCA	0.028	7.67	0.0096	1.40E-10	2.10E-11	5.20E-15	70.5	76	87.5	90.3	0.024	0.023	0.0079	3
F	COAD	0.033	7.59	0.0095	4.00E-12	2.30E-12	5.80E-16	288	291	87.5	91.4	0.088	0.091	0.0088	9.9
F	COADREAD	0.032	7.25	0.0094	2.30E-12	1.50E-12	5.90E-16	334	335	87.5	91.2	0.1	0.11	0.0094	11
F	ESCA	0.022	7.32	0.0097	1.80E-07	6.70E-09	2.10E-12	14.7	15.5	87.5	88.8	0.0054	0.0048	0.0077	0.7
F	GBM	0.015	5.61	0.0102	1.10E-07	4.50E-09	6.00E-16	11.9	10.5	77.5	80.8	0.0038	0.0039	0.0074	0.51
F	HNSC	0.018	5.66	0.0097	4.20E-08	2.60E-09	2.20E-13	30.6	31.6	77.5	84.6	0.013	0.012	0.0093	1.4
F	KICH	0.0098	5.57	0.0105	4.20E-04	4.30E-06	1.20E-13	0.996	0.863	82.5	78	0.00033	0.00031	0.0061	0.054
F	KIRC	0.011	4.54	0.0104	6.10E-05	3.60E-06	4.10E-15	11.6	9.78	72.5	74.7	0.0038	0.0041	0.0081	0.46
F	KIRP	0.0098	5.44	0.0105	5.70E-05	4.90E-07	1.80E-14	1.45	1.16	77.5	77.8	0.00043	0.00042	0.0064	0.067
F	LAML	0.02	6.76	0.0096	1.70E-11	7.00E-13	9.30E-17	20.4	19.5	87.5	88.4	0.007	0.0066	0.0086	0.8
F	LGG	0.00052	2.06	0.0089	4.30E-01	1.00E-01	1.50E-05	2.58	0.59	102.5	57.8	0.0007	0.00044	0.021	0.034
F	LIHC	0.019	6.63	0.0102	3.90E-07	2.30E-08	2.60E-15	11.2	11.5	77.5	82.9	0.0039	0.0037	0.0058	0.67
F	LUAD	0.025	6.06	0.0102	1.20E-06	7.20E-07	8.60E-14	117	104	77.5	81.8	0.036	0.036	0.0066	5.5
F	LUSC	0.026	7.15	0.0103	1.80E-05	5.20E-06	9.40E-14	54.1	44.8	77.5	83.6	0.014	0.014	0.0052	2.8
F	MESO	0.02	7.99	0.0102	4.90E-07	1.10E-08	1.80E-16	2.38	1.99	82.5	85.4	0.00055	0.00055	0.0047	0.12
F	PAAD	0.023	6.68	0.0099	1.60E-07	3.40E-08	5.80E-15	43.6	43.2	77.5	85.6	0.014	0.014	0.0071	1.9
F	PCPG	0.0015	3.24	0.0108	4.40E-01	7.90E-02	2.40E-08	0.141	0.0863	72.5	64	5.00E-05	4.30E-05	0.01	0.0049
F	READ	0.019	5.85	0.0093	1.90E-12	1.10E-13	1.80E-16	46.6	45.1	87.5	89	0.017	0.018	0.012	1.5
F	SARC	0.0057	4.25	0.0054	1.50E-01	7.00E-03	3.10E-01	5.54	8.09	97.5	143	0.0016	0.0069	0.15	0.011
F	SKCM	0.0085	3.43	0.0078	5.50E-06	1.80E-07	2.70E-08	42.1	42.3	82.5	91	0.024	0.028	0.03	0.79
F	STAD	0.026	7.62	0.0094	9.30E-11	6.20E-12	1.20E-14	44.7	44.6	87.5	92.5	0.014	0.014	0.0096	1.4
F	THCA	0.0033	2.15	0.0098	1.40E-10	2.00E-12	2.90E-20	20.7	20.3	52.5	54.7	0.012	0.014	0.017	0.73
F	THYM	0.007	5	0.0104	8.40E-03	1.00E-04	4.00E-11	0.724	0.502	72.5	76.6	0.00021	0.0002	0.0073	0.029
F	BRCA	0.022	3.43	0.0112	2.30E-11	1.10E-10	6.30E-15	454	440	77.5	78	0.2	0.2	0.0084	24
F	CESC	0.0013	1.6	0.0098	6.50E-05	1.70E-06	9.10E-11	15.5	14.5	42.5	53.2	0.0095	0.01	0.015	0.64
F	OV	0.008	4	0.0122	5.30E-06	3.90E-08	1.60E-14	4.34	4.08	77.5	76.6	0.0016	0.0016	0.0051	0.31
F	UCEC	0.014	3.62	0.0119	9.50E-07	2.20E-07	5.50E-13	74.4	74.3	67.5	76	0.031	0.032	0.0065	4.8
F	UCS	0.0067	4.96	0.0121	8.70E-04	1.50E-06	7.70E-11	0.426	0.237	97.5	81.2	9.80E-05	8.00E-05	0.0036	0.027

⁰Female reproductive cancers: BRCA breast invasive carcinoma, CESC cervical squamous cell carcinoma and endocervical adenocarcinoma, OV ovarian serous cystadenocarcinoma, UCEC uterine corpus endometrial carcinoma, UCS uterine carcinosarcoma.

Abbreviations for non-reproductive cancer types and footnotes 1-4 are explained in Supplementary Table 2A. ACC, LGG, PCPG and SARC are cancer types with *P* values for model-fitted u_{μ} or *k* larger than 0.1 and were omitted from further analysis.

Supplementary Table 2C. Both sexes pooled (M&F) parameter values of model-fits to SEER 2000–2003 age-specific cancer incidence rates for non-reproductive cancer types only, employing the multistage-senescence model (Equation 5).

Sex	Cancer type (TCGA) ⁰	Model-fitted ¹			<i>P</i> values			Peak incidence rate (per 100,000 person-year)		Age of peak incidence (yr)		Cumulative probability over lifespan			Ratio of cum. prob., SEER/2-variable
		u_{μ} (yr ⁻¹)	<i>k</i>	<i>b</i> (yr ⁻¹)	<i>u</i>	<i>k</i>	<i>b</i>	SEER	Model-fitted ²	SEER	Model-fitted ³	SEER	Model-fitted	2-Variable model fitted ⁴	
M&F	ACC	0.0036	4.01	0.0104	1.20E-01	4.20E-03	2.70E-08	0.343	0.246	62.5	72	0.00013	0.00011	0.0047	0.027
M&F	BLCA	0.032	7.64	0.0097	1.60E-09	6.60E-10	5.70E-14	153	171	82.5	89.5	0.051	0.052	0.015	3.3
M&F	COAD	0.033	7.44	0.0095	1.10E-11	6.40E-12	3.70E-15	307	321	87.5	91.5	0.096	0.1	0.018	5.4
M&F	COADREAD	0.032	7.06	0.0094	5.60E-12	3.90E-12	2.90E-15	363	372	87.5	90.9	0.12	0.12	0.016	7.1
M&F	ESCA	0.021	6.37	0.01	5.20E-08	3.60E-09	9.10E-14	24.5	27.2	82.5	84.5	0.01	0.0092	0.0099	1
M&F	GBM	0.016	5.62	0.0101	1.50E-07	7.50E-09	3.30E-15	14.8	13.6	77.5	81.1	0.0049	0.005	0.0078	0.62
M&F	HNSC	0.017	4.92	0.0099	2.50E-07	3.80E-08	5.50E-13	53.4	55.1	72.5	80.4	0.023	0.023	0.0076	3.1
M&F	KICH	0.011	5.66	0.0105	1.60E-06	1.10E-08	2.70E-16	1.36	1.19	77.5	78.5	0.00043	0.00042	0.0065	0.066
M&F	KIRC	0.012	4.58	0.0104	1.80E-05	1.40E-06	2.70E-15	16.2	13.8	72.5	75.5	0.0053	0.0058	0.0057	0.93
M&F	KIRP	0.011	5.18	0.0105	3.00E-05	4.90E-07	2.30E-15	2.94	2.65	72.5	76.9	0.00094	0.001	0.006	0.16
M&F	LAML	0.024	7.33	0.0098	1.10E-11	6.90E-13	4.20E-17	26.2	26.4	87.5	88.1	0.0088	0.0082	0.013	0.66
M&F	LGG	0.00099	2.37	0.0094	2.80E-01	3.70E-02	4.70E-07	2.05	0.73	102.5	61.3	0.00074	0.00049	0.00051	1.5
M&F	LIHC	0.015	5.17	0.0102	6.00E-08	3.90E-09	1.10E-15	19.9	18.9	77.5	79.4	0.0072	0.0074	0.0071	1
M&F	LUAD	0.027	6.39	0.0102	7.20E-07	4.50E-07	1.90E-13	138	127	77.5	83.1	0.042	0.042	0.0089	4.7
M&F	LUSC	0.028	7.19	0.0102	6.90E-06	2.90E-06	1.90E-13	89.3	76.3	77.5	84.1	0.024	0.023	0.0095	2.5
M&F	MESO	0.026	8.92	0.0102	1.00E-07	4.60E-09	4.20E-15	6.28	6.32	82.5	87.2	0.0017	0.0016	0.013	0.13
M&F	PAAD	0.024	6.66	0.01	8.40E-08	1.60E-08	1.50E-14	48.3	48.4	77.5	84.7	0.015	0.016	0.01	1.5
M&F	PCPG	9.70E-08	0.77	0.005	9.90E-01	9.50E-01	8.60E-01	0.132	NaN	67.5	-59.4	5.70E-05	0.00014	NaN	NaN
M&F	READ	0.021	5.9	0.0096	2.90E-12	2.80E-13	6.90E-17	55.5	56	87.5	86.2	0.021	0.021	0.011	1.9
M&F	SARC	0.012	5.87	0.0086	2.00E-04	1.40E-06	7.20E-07	5.99	5.14	97.5	96.4	0.0018	0.0022	0.021	0.085
M&F	SKCM	0.016	4.73	0.0092	8.40E-11	7.70E-12	1.30E-14	70.8	69.6	82.5	85.6	0.033	0.032	0.01	3.2
M&F	STAD	0.026	7.3	0.0095	1.70E-12	1.50E-13	2.10E-16	56.4	59.6	87.5	90.7	0.02	0.019	0.016	1.2
M&F	THCA	0.0046	2.67	0.0097	4.80E-07	2.20E-08	2.20E-15	15.6	15.1	67.5	64.2	0.0092	0.0093	0.0017	5.2
M&F	THYM	0.0079	5.18	0.0104	5.70E-05	2.30E-07	5.60E-14	0.729	0.612	72.5	77.3	0.00025	0.00023	0.0062	0.04

⁰Abbreviations for non-reproductive cancer types and footnotes 1-4 are explained in Supplementary Table 2A. ACC, LGG, and PCPG are cancer types with *P* values for model-fitted u_{μ} or *k* larger than 0.1 and were omitted from further analysis.

Supplementary Table 3. Correspondence of cancer types in TCGA and SEER, from Wang et al. (2018).

TCGA code	TCGA cancer type	SEER ICD-O-3 site (histology) code
ACC	Adrenocortical carcinoma	C74.0-C74.9 (8370/3)
BLCA	Bladder urothelial carcinoma	C67.0-C67.9 (8050, 8120, 8130, 8131)
BRCA	Breast invasive carcinoma	C50.0-C50.9 (801-857)
CESC	Cervical squamous cell carcinoma and endocervical adenocarcinoma	C53.0-C53.9 (807, 814-857)
COAD	Colon adenocarcinoma	C18.0-C18.9 (814-857)
ESCA	Esophageal carcinoma	C15.0-C15.9 (801-857)
GBM	Glioblastoma multiforme	(9440/3)
HNSC	Head and neck squamous cell carcinoma	C00.0-C15.0, C15.3, C30.0, C31.0-C33.9, C41.0, C41.1, C47.0, C49.0, C73.9, C75.4 C77.0 (807)
KICH	Kidney chromophobe	C64.9, C65.9 (8317, 8270)
KIRC	Kidney renal clear cell carcinoma	C64.9, C65.9 (8310/3)
KIRP	Kidney renal papillary cell carcinoma	C64.9, C65.9 (8260)
LAML	Acute myeloid leukemia	ICCC site recode ICD-O-3/WHO 2008=I(b) Acute myeloid leukemias
LGG	Brain lower grade glioma	C71.0-C71.9 (9380-9384, 9391-9460, Grade I and II)
LIHC	Liver hepatocellular carcinoma	C22.0 (817-818)
LUAD	Lung adenocarcinoma	C34.0-C34.9 (814-857)
LUSC	Lung squamous cell carcinoma	C34.0-C34.9 (807)
MESO	Mesothelioma	(905)
OV	Ovarian serous cystadenocarcinoma	C56.9 (8441.3)
PAAD	Pancreatic adenocarcinoma	C25.0-C25.9 (814-857)
PCPG	Pheochromocytoma and paraganglioma	(868, 869, 870)
PRAD	Prostate adenocarcinoma	C61.9 (814-857)
READ	Rectum adenocarcinoma	C61.9 (814-857)
SARC	Sarcoma	(880)
SKCM	Skin cutaneous melanoma	C44.0-C44.9 (8720-8790)
STAD	Stomach adenocarcinoma	C16.0-C16.9 (814-857)
TGCT	Testicular germ cell tumors	C62.0-C62.9 (9060-9100)
THCA	Thyroid carcinoma	C73.9 (801-857)
THYM	Thymoma	C37.9 (8580-8585)
UCEC	Uterine corpus endometrial carcinoma	C54.0-C54.9 (8140, 8380, 8382, 8480, 8482, 8560, 8570, 8310, 8441, 8460, 8260)
UCS	Uterine carcinosarcoma	C55.9 (8980-8981)

Red and blue text for female and male reproductive cancers, respectively.

Supplementary Table 4A. Male (M) parameter values of fits to SEER 2010-2013 age-specific cancer incidence rates employing the multistage-senescence model of Equation 4 (Pompei and Wilson, 2001; Harding et al. 2008).

Sex	Cancer type	Model -fitted			Peak incidence rate (per 100,000 person-year)		Age of peak incidence (yr)		Cumulative probability over lifespan	
		<i>a</i>	<i>k</i>	<i>b</i> (yr ⁻¹)	SEER	Model-fitted	SEER	Model-fitted	SEER	Model-fitted
M	All Major	1.48E-12	6.75	0.0099	2682.3	2943.1	92.5	86.1	1.103	0.965
M	All Major Non Sex	6.07E-13	6.86	0.0096	2243.7	2326.6	92.5	89.2	0.837	0.778
M	All Sites	1.50E-12	6.76	0.0098	3016.5	3220.0	92.5	86.7	1.205	1.062
M	Brain and Other Nervous System	2.70E-12	5.54	0.0097	40.1	27.7	102.5	84.4	0.014	0.011
M	Colon and Rectum	6.42E-12	5.77	0.0083	354.6	372.2	92.5	99.4	0.125	0.164
M	Esophagus	1.47E-14	6.88	0.0100	44.3	48.6	92.5	85.5	0.017	0.016
M	¹ Hodgkin Lymphoma	2.45E-07	2.20	0.0000	5.4	NA	87.5	Inf	0.003	Inf
M	Kidney and Renal Pelvis	2.82E-12	5.85	0.0100	92.1	99.5	77.5	83.0	0.041	0.036
M	Larynx	1.35E-13	6.30	0.0102	29.0	31.5	77.5	82.7	0.012	0.011
M	Leukemia	2.22E-15	7.44	0.0094	143.4	140.1	92.5	92.5	0.047	0.045
M	Liver and Intrahepatic Bile Duct	1.91E-10	4.77	0.0099	56.7	58.5	82.5	79.7	0.024	0.025
M	Lung and Bronchus	4.60E-16	8.22	0.0101	512.1	563.0	82.5	87.2	0.172	0.155
M	Melanoma of the Skin	2.83E-13	6.42	0.0091	230.4	206.8	102.5	93.2	0.077	0.077
M	Myeloma	6.37E-16	7.63	0.0099	59.0	64.6	82.5	87.7	0.019	0.019
M	Non-Hodgkin Lymphoma	3.34E-14	6.90	0.0095	160.5	159.3	92.5	89.8	0.055	0.053
M	Oral Cavity and Pharynx	8.44E-10	4.43	0.0095	100.2	68.6	102.5	81.4	0.035	0.032
M	Pancreas	3.33E-15	7.36	0.0096	116.2	117.6	92.5	89.6	0.039	0.037
M	Stomach	6.10E-15	7.11	0.0094	84.6	80.8	97.5	91.5	0.027	0.027
M	Thyroid	1.58E-09	4.02	0.0103	18.2	17.0	72.5	73.2	0.008	0.008
M	Urinary Bladder	6.02E-18	9.05	0.0097	396.7	416.6	92.5	91.8	0.122	0.110
M	Prostate	6.57E-10	5.27	0.0124	749.7	691.7	72.5	80.1	0.261	0.218
M	Testis	5.23E-05	1.49	0.0236	15.1	12.8	27.5	29.0	0.004	0.004

NA Not Available; Inf Infinity.

¹Hodgkin's lymphoma has a bimodal, rather than a unimodal distribution, thus does not well fit the multistage-senescence model.

The peak age-specific incidence rate, age of peak incidence, and cumulative probability over life span are computed up to maximum age 105, based on the SEER data alternatively model-fitted $ASR(t)$.

Supplementary Table 4B. Female (F) parameter values of fits to SEER 2010-2013 age-specific cancer incidence rates employing the multistage-senescence model of Equation 4 (Pompei and Wilson, 2001; Harding et al. 2008).

Sex	Cancer type	Model -fitted			Peak incidence rate (per 100,000 person-year)		Age of peak incidence (yr)		Cumulative probability over lifespan	
		<i>a</i>	<i>k</i>	<i>b</i> (yr ⁻¹)	SEER	Model-fitted	SEER	Model-fitted	SEER	Model-fitted
F	All Major	2.51E-10	5.43	0.0095	1684.0	1740.1	82.5	85.9	0.739	0.702
F	All Major Non Sex	2.71E-12	6.37	0.0095	1161.7	1224.0	82.5	88.6	0.467	0.437
F	All Sites	2.28E-10	5.47	0.0094	1860.1	1936.8	82.5	86.9	0.821	0.785
F	Brain and Other Nervous System	8.51E-12	5.17	0.0095	17.8	17.9	77.5	84.8	0.009	0.007
F	Colon and Rectum	1.80E-12	6.00	0.0083	281.6	304.7	92.5	100.8	0.094	0.131
F	Esophagus	1.16E-15	7.10	0.0096	16.1	13.2	102.5	89.7	0.005	0.004
F	¹ Hodgkin Lymphoma	1.92E-11	4.61	0.0096	4.4	3.3	22.5	81.7	0.002	0.001
F	Kidney and Renal Pelvis	3.74E-12	5.61	0.0098	46.6	48.0	77.5	83.8	0.021	0.018
F	Larynx	2.69E-11	4.65	0.0102	5.1	4.5	77.5	77.0	0.002	0.002
F	Leukemia	9.14E-15	6.97	0.0092	80.3	74.3	102.5	93.3	0.027	0.026
F	Liver and Intrahepatic Bile Duct	9.93E-14	6.29	0.0097	27.9	28.0	82.5	86.5	0.010	0.010
F	Lung and Bronchus	1.15E-14	7.37	0.0100	335.2	342.6	82.5	86.4	0.110	0.104
F	Melanoma of the Skin	3.14E-09	3.98	0.0080	60.7	61.0	87.5	94.1	0.029	0.036
F	Myeloma	1.03E-14	6.87	0.0099	34.3	34.7	82.5	86.1	0.012	0.011
F	Non-Hodgkin Lymphoma	4.61E-14	6.74	0.0097	96.3	98.4	82.5	87.7	0.035	0.033
F	Oral Cavity and Pharynx	7.32E-11	4.70	0.0082	37.1	33.1	92.5	95.8	0.014	0.017
F	Pancreas	4.26E-16	7.77	0.0095	104.1	107.5	92.5	92.0	0.034	0.033
F	Stomach	9.39E-15	6.82	0.0091	48.2	42.2	102.5	94.1	0.015	0.015
F	Thyroid	4.22E-06	2.31	0.0103	37.7	35.6	52.5	55.3	0.021	0.022
F	Urinary Bladder	8.90E-17	8.08	0.0095	80.2	85.3	92.5	91.8	0.027	0.025
F	Breast	2.33E-07	3.67	0.0113	436.5	436.2	77.5	79.6	0.205	0.194
F	Cervix Uteri	3.10E-05	1.50	0.0093	14.4	12.5	42.5	50.9	0.008	0.009
F	Corpus Uteri	1.13E-07	3.50	0.0120	100.8	89.2	67.5	74.4	0.037	0.038
F	Ovary	1.48E-08	3.74	0.0102	48.2	47.8	87.5	87.0	0.022	0.023

¹Hodgkin's lymphoma has a bimodal, rather than a unimodal distribution, thus does not well fit the multistage-senescence model.

Supplementary Table 4C. Male and female pooled (M&F) parameter values of fits to SEER 2010-2013 age-specific cancer incidence rates employing the multistage-senescence model of Equation 4 (Pompei and Wilson, 2001; Harding et al. 2008).

Sex	Cancer type	Model -fitted			Peak incidence rate (per 100,000 person- year)		Age of peak incidence (yr)		Cumulative probability over lifespan	
		<i>a</i>	<i>k</i>	<i>b</i> (yr ⁻¹)	SEER	Model-fitted	SEER	Model-fitted	SEER	Model-fitted
M&F	All Major	2.06E-11	6.08	0.0098	2052.5	2219.4	82.5	85.6	0.865	0.800
M&F	All Major Non Sex	1.51E-12	6.58	0.0096	1544.7	1633.9	82.5	87.9	0.598	0.561
M&F	All Sites	1.89E-11	6.11	0.0097	2253.5	2439.4	82.5	86.2	0.953	0.881
M&F	Brain and Other Nervous System	5.92E-12	5.31	0.0097	21.8	21.9	77.5	84.1	0.011	0.009
M&F	Colon and Rectum	3.68E-12	5.87	0.0084	303.9	315.8	92.5	98.3	0.105	0.135
M&F	Esophagus	2.27E-14	6.64	0.0099	24.6	27.0	82.5	85.4	0.010	0.009
M&F	¹ Hodgkin Lymphoma	2.69E-10	4.01	0.0092	4.3	3.8	77.5	81.9	0.003	0.002
M&F	Kidney and Renal Pelvis	5.55E-12	5.61	0.0099	66.4	68.9	77.5	82.7	0.029	0.026
M&F	Larynx	1.34E-12	5.62	0.0102	15.5	15.4	77.5	80.8	0.006	0.006
M&F	Leukemia	4.94E-15	7.19	0.0094	93.8	96.2	92.5	91.4	0.035	0.032
M&F	Liver and Intrahepatic Bile Duct	5.20E-11	4.97	0.0098	39.6	39.8	82.5	81.4	0.016	0.017
M&F	Lung and Bronchus	3.69E-15	7.68	0.0100	406.8	425.9	82.5	86.8	0.131	0.124
M&F	Melanoma of the Skin	5.96E-12	5.62	0.0092	108.8	109.8	92.5	89.1	0.045	0.044
M&F	Myeloma	3.67E-15	7.17	0.0099	44.3	46.0	82.5	86.6	0.015	0.014
M&F	Non-Hodgkin Lymphoma	4.43E-14	6.80	0.0097	115.9	120.5	82.5	87.9	0.042	0.040
M&F	Oral Cavity and Pharynx	7.25E-10	4.35	0.0092	47.5	45.4	92.5	83.3	0.022	0.022
M&F	Pancreas	1.83E-15	7.46	0.0095	107.7	111.0	92.5	91.0	0.036	0.035
M&F	Stomach	1.05E-14	6.90	0.0094	53.4	55.2	92.5	91.1	0.020	0.019
M&F	Thyroid	1.06E-06	2.56	0.0100	27.3	25.4	67.5	60.8	0.015	0.015
M&F	Urinary Bladder	3.08E-17	8.54	0.0098	181.0	201.9	87.5	90.3	0.059	0.055

¹Hodgkin's lymphoma has a bimodal, rather than a unimodal distribution, thus does not well fit the multistage-senescence model.

Supplementary Table 5A. Male (M) parameter values of fits to SEER 2000-2003 age-specific cancer incidence rates employing the multistage-senescence model of Equation 4 (Pompei and Wilson, 2001; Harding et al. 2008).

Sex	Cancer type	Model -fitted			Peak incidence rate (per 100,000 person- year)		Age of peak incidence (yr)		Cumulative probability over lifespan	
		<i>a</i>	<i>k</i>	<i>b</i> (yr ⁻¹)	SEER	Model-fitted	SEER	Model-fitted	SEER	Model-fitted
M	All Major	5.29E-12	6.45	0.0093	3172.4	3755.9	87.5	90.5	1.236	1.353
M	All Major Non Sex	2.23E-12	6.55	0.0092	2333.2	2591.7	87.5	91.6	0.844	0.931
M	All Sites	5.44E-12	6.45	0.0093	3462.7	4087.6	87.5	91.1	1.337	1.481
M	Brain and Other Nervous System	3.67E-12	5.49	0.0099	27.0	27.5	77.5	83.0	0.012	0.011
M	Colon and Rectum	3.74E-14	7.11	0.0094	520.6	522.4	92.5	91.9	0.164	0.174
M	Esophagus	6.44E-14	6.55	0.0100	50.2	49.1	102.5	84.9	0.019	0.016
M	¹ Hodgkin Lymphoma	3.13E-10	4.07	0.0098	7.7	4.7	97.5	77.0	0.003	0.002
M	Kidney and Renal Pelvis	2.69E-12	5.82	0.0099	82.0	86.3	87.5	83.5	0.035	0.032
M	Larynx	1.17E-12	5.84	0.0102	33.4	35.4	72.5	81.2	0.013	0.013
M	Leukemia	3.38E-15	7.34	0.0093	136.0	138.5	92.5	92.8	0.046	0.045
M	Liver and Intrahepatic Bile Duct	2.21E-11	5.16	0.0095	43.3	44.3	77.5	84.5	0.018	0.018
M	Lung and Bronchus	1.60E-14	7.43	0.0099	563.9	644.4	77.5	87.4	0.198	0.196
M	Melanoma of the Skin	2.48E-11	5.29	0.0089	126.6	124.8	92.5	91.6	0.050	0.055
M	Myeloma	2.38E-15	7.29	0.0098	54.2	56.0	87.5	88.3	0.019	0.018
M	Non-Hodgkin Lymphoma	2.13E-13	6.45	0.0094	149.9	142.7	87.5	89.5	0.051	0.051
M	Oral Cavity and Pharynx	1.19E-09	4.32	0.0092	69.8	65.0	92.5	83.1	0.031	0.032
M	Pancreas	3.48E-15	7.33	0.0096	100.1	106.7	92.5	89.6	0.035	0.034
M	Stomach	2.01E-15	7.40	0.0094	120.4	101.8	102.5	92.0	0.036	0.033
M	Thyroid	1.80E-09	3.87	0.0102	10.9	10.2	67.5	72.4	0.005	0.005
M	Urinary Bladder	2.18E-16	8.21	0.0095	349.7	393.1	87.5	92.2	0.108	0.114
M	Prostate	2.90E-10	5.52	0.0118	1034.0	1107.3	72.5	84.5	0.388	0.356
M	Testis	3.11E-05	1.66	0.0237	12.9	12.0	32.5	31.7	0.004	0.003

¹Hodgkin's lymphoma has a bimodal, rather than a unimodal distribution, thus does not well fit the multistage-senescence model.

The peak age-specific incidence rate, age of peak incidence, and cumulative probability over life span are computed up to maximum age 105, based on the SEER data alternatively model-fitted $ASR(t)$.

Supplementary Table 5B. Female (F) parameter values of fits to SEER 2000-2003 age-specific cancer incidence rates employing the multistage-senescence model of Equation 4 (Pompei and Wilson, 2001; Harding et al. 2008).

Sex	Cancer type	Model -fitted			Peak incidence rate (per 100,000 person- year)		Age of peak incidence (yr)		Cumulative probability over lifespan	
		<i>a</i>	<i>k</i>	<i>b</i> (yr ⁻¹)	SEER	Model-fitted	SEER	Model-fitted	SEER	Model-fitted
F	All Major	5.28E-10	5.26	0.0093	1801.6	1861.2	87.5	87.5	0.771	0.789
F	All Major Non Sex	3.68E-12	6.30	0.0093	1262.8	1333.5	87.5	90.2	0.481	0.490
F	All Sites	4.53E-10	5.31	0.0092	2020.8	2074.8	87.5	88.5	0.853	0.882
F	Brain and Other Nervous System	6.62E-12	5.25	0.0098	18.8	17.8	77.5	82.6	0.008	0.007
F	Colon and Rectum	1.91E-14	7.18	0.0092	408.6	415.3	92.5	93.9	0.129	0.140
F	Esophagus	4.98E-16	7.34	0.0096	16.6	16.4	97.5	89.7	0.006	0.005
F	¹ Hodgkin Lymphoma	1.51E-11	4.67	0.0097	4.5	3.3	22.5	81.4	0.002	0.001
F	Kidney and Renal Pelvis	1.90E-12	5.73	0.0098	41.6	42.3	82.5	84.1	0.016	0.016
F	Larynx	6.35E-12	5.05	0.0104	6.7	5.4	72.5	76.9	0.002	0.002
F	Leukemia	8.77E-15	6.97	0.0091	75.0	75.5	97.5	94.1	0.026	0.026
F	Liver and Intrahepatic Bile Duct	3.37E-15	7.02	0.0098	23.2	22.9	102.5	87.4	0.009	0.007
F	Lung and Bronchus	2.33E-13	6.69	0.0100	325.5	324.0	77.5	84.9	0.110	0.106
F	Melanoma of the Skin	3.88E-08	3.31	0.0074	42.9	43.1	87.5	94.4	0.024	0.031
F	Myeloma	7.30E-15	6.93	0.0099	32.9	33.3	87.5	86.8	0.010	0.011
F	Non-Hodgkin Lymphoma	1.58E-13	6.45	0.0096	99.2	98.0	87.5	87.8	0.036	0.034
F	Oral Cavity and Pharynx	5.98E-12	5.34	0.0091	46.5	32.7	102.5	89.6	0.015	0.014
F	Pancreas	3.28E-16	7.81	0.0095	100.1	99.8	92.5	92.1	0.031	0.030
F	Stomach	6.67E-16	7.46	0.0091	56.3	56.1	92.5	95.5	0.017	0.019
F	Thyroid	5.26E-06	2.10	0.0099	20.3	19.7	52.5	52.9	0.012	0.013
F	Urinary Bladder	5.19E-16	7.68	0.0095	81.4	87.3	87.5	91.8	0.028	0.027
F	Breast	8.29E-07	3.35	0.0109	458.3	449.7	77.5	79.4	0.218	0.218
F	Cervix Uteri	3.31E-05	1.53	0.0087	16.4	15.3	42.5	54.8	0.011	0.012
F	Corpus Uteri	5.53E-08	3.65	0.0117	85.2	86.5	67.5	77.1	0.037	0.037
F	Ovary	6.60E-09	4.02	0.0110	58.7	57.4	82.5	83.4	0.025	0.025

¹Hodgkin's lymphoma has a bimodal, rather than a unimodal distribution, thus does not well fit the multistage-senescence model.

Supplementary Table 5C. Male and female pooled (M&F) parameter values of fits to SEER 2000-2003 age-specific cancer incidence rates employing the multistage-senescence model of Equation 4 (Pompei and Wilson, 2001; Harding et al. 2008).

Sex	Cancer type	Model -fitted			Peak incidence rate (per 100,000 person- year)		Age of peak incidence (yr)		Cumulative probability over lifespan	
		<i>a</i>	<i>k</i>	<i>b</i> (yr ⁻¹)	SEER	Model-fitted	SEER	Model-fitted	SEER	Model-fitted
M&F	All Major	9.45E-11	5.71	0.0093	2254.2	2522.2	87.5	88.9	0.933	1.003
M&F	All Major Non Sex	7.20E-12	6.20	0.0093	1614.0	1764.7	87.5	90.7	0.610	0.661
M&F	All Sites	8.77E-11	5.74	0.0092	2494.1	2775.2	87.5	89.7	1.021	1.107
M&F	Brain and Other Nervous System	7.17E-12	5.28	0.0099	22.2	21.6	77.5	82.3	0.010	0.009
M&F	Colon and Rectum	5.30E-14	6.98	0.0092	438.3	452.9	87.5	93.1	0.143	0.156
M&F	Esophagus	8.33E-14	6.35	0.0099	25.5	28.0	87.5	85.2	0.010	0.010
M&F	¹ Hodgkin Lymphoma	1.55E-10	4.17	0.0097	4.3	3.8	27.5	78.6	0.003	0.002
M&F	Kidney and Renal Pelvis	5.19E-12	5.59	0.0099	56.9	59.1	77.5	83.0	0.023	0.022
M&F	Larynx	6.89E-12	5.28	0.0103	18.6	17.1	72.5	79.0	0.006	0.007
M&F	Leukemia	8.67E-15	7.05	0.0093	90.5	94.8	87.5	92.1	0.033	0.032
M&F	Liver and Intrahepatic Bile Duct	3.58E-12	5.50	0.0097	28.9	30.3	77.5	84.6	0.012	0.012
M&F	Lung and Bronchus	1.41E-13	6.85	0.0099	424.1	431.6	77.5	86.0	0.141	0.139
M&F	Melanoma of the Skin	2.57E-10	4.67	0.0091	69.8	69.4	82.5	86.3	0.033	0.033
M&F	Myeloma	5.48E-15	7.05	0.0099	39.9	41.2	87.5	86.9	0.013	0.013
M&F	Non-Hodgkin Lymphoma	2.43E-13	6.39	0.0096	115.8	113.0	87.5	87.9	0.042	0.040
M&F	Oral Cavity and Pharynx	4.56E-10	4.45	0.0093	45.1	44.1	102.5	83.8	0.021	0.021
M&F	Pancreas	1.98E-15	7.42	0.0095	100.0	102.1	92.5	91.4	0.033	0.032
M&F	Stomach	3.12E-15	7.21	0.0093	67.9	69.5	92.5	92.3	0.023	0.023
M&F	Thyroid	6.51E-07	2.53	0.0098	14.7	14.3	67.5	62.0	0.009	0.009
M&F	Urinary Bladder	1.24E-15	7.68	0.0096	169.3	186.3	87.5	90.5	0.055	0.057

¹Hodgkin's lymphoma has a bimodal, rather than a unimodal distribution, thus does not well fit the multistage-senescence model.

Supplementary Notes

Please browse Full Text version to see the Supplementary Notes.